Chemi-ionization processes

A. N. Klyucharev

St. Petersburg State University
(Submitted 2 November 1992; resubmitted after revision 25 February 1993)
Usp. Fiz. Nauk. **163**, 39–73 (June 1993)

A systematic presentation is given of the current state of experimental and theoretical studies of elementary processes involved in chemi-ionization by collision between atoms and molecules at thermal energies. General conclusions are presented about the rates of these processes, their importance in practical applications, and their effect on the macroscopic properties of the medium in which they take place. The review is intended for research workers and for postgraduate and graduate students specializing in plasma physics, atom-molecule collisions, and the interaction between radiation and matter.

INTRODUCTION

Papers on chemi-ionization processes began to appear in the physics literature in the early 1970s (cf. Refs. 1-4). They signalled the beginning of extensive experimental and theoretical studies of chemi-ionization at several scientific centers, and the realization of the practical implications of the basic research that began abroad in the 1930s (Ref. 5) during a period that in many ways determined the subsequent course of modern physics as a whole. Despite the large volume of material that has already been published, interest in these studies continues unabated. By studying the physics of chemi-ionization processes, researchers are exploring the fundamental assumptions of the theory of atomic collisions and the physics of low-temperature plasmas, and hence the possibility of new phenomena and new properties. One such result has been the discovery of photoresonant plasma, formed when a gaseous medium is exposed to light with wavelengths corresponding to resonant transitions in the corresponding atoms. The process responsible for this plasma cannot be described in terms of the relationships that are familiar in gas-discharge physics. This has, in turn, led to a new research field in the study of highly-ionized plasmas in zero electric and magnetic fields. Such plasmas have extreme properties as compared with equilibrium gas-discharge plasmas. Chemi-ionization research has led to advances in optogalvanic spectroscopy, the emergence of new methods for controlling plasmas with external light, studies of many-particle interactions and their effect on the thermodynamic properties of plasmas, the development of new systems for the nonlinear transformation and stabilization radiation frequency, ion doping and etching, and so on.

Chemi-ionization is discussed to a greater or lesser extent in a number of research monographs (cf., for example, Ref. 2). However, because of lack of space, these publications have not adequately explored a number of controversial topics in chemi-ionization. On the other hand, more specialized review papers tend to reflect the professional interests of their authors and do not therefore set the subject in its general context. Moreover, before they can be used, the data assembled by different authors on chemi-ionization rate constants require preliminary methodological analysis. This is so, above all, because many of the experiments have been performed without allowing for the fact that the colliding-particle velocity distributions were not equilibrium distributions. In particular, this has meant that chemi-ionization data obtained in beam experiments could not be used under the conditions prevailing in plasmas.

The aim of this review is to fill, as fully as possible, this gap in the physics literature.

2. CLASSIFICATION OF CHEMI-IONIZATION PROCESSES INVOLVING HEAVY PARTICLES WITH THERMAL ENERGIES

2.1. Depending on the state of the colliding particles

Depending on the state of the colliding particles in the entrance and exit channels of a particular reaction, the ionization processes accompanying collisions between atoms and molecules can generally be divided into ionization by impact (ionizing collisions) and chemi-ionization. This somewhat arbitrary subdivision is dictated mostly by the ratio of the potential energy (excitation energy) of the colliding particles to their kinetic energy (energy of relative motion).

In a wide range of thermal and subthermal collision velocities, ionization implies the formation of an intermediate quasimolecular complex with specific 'chemical' bonding. The stabilization of this complex or its decay with the formation of charged fragments is determined by factors such as the nature of the colliding particles, their degree of excitation, and the properties of the atomic interaction potential. Kinetic energy plays a basic role in ionization by collision, whereas chemi-ionization is determined by the character of the excitation of the colliding particles. Chemi-ionization processes are of immediate interest in the physics and chemistry of plasmas. In these processes, transitions to the continuum occur mostly at the expense of internal excitation energy, and ionization leads to a change in the particle structure, i.e., to a redistribution of the outer electrons in the colliding particles:

$$X+Y\rightarrow XY^{+}+e. \tag{2.1}$$

 1063-7869/93/060486-27$10.00

Chemi-ionization reactions are traditionally regarded in plasma physics as an effective channel for the production of molecular ions. Charged-particle production channels become active even when atoms are excited to the lowest-lying (resonant) states:

$$X^* + X^* \rightarrow X_2^+ + e(AI), \tag{2.2}$$

$$X^* + X^* \rightarrow X^+ + X + e(PI). \tag{2.3}$$

Two ionization channels are possible in binary collisions such as (2.2) and (2.3) between excited particles, namely, associative ionization (AI) and Penning ionization (PI), These reactions are of particular interest in practical applications because they can produce charged particles for a minimum expenditure of energy by the external source. Reaction (2.2) is sometimes referred to in the literature as Penning associative ionization (PAI) whereas AI with the participation of an excited and a ground-state atom is called Hornbeck–Molnar ionization (HMI).

Collisions that involve excited atoms and result in their ionization are accompanied by an interaction of the initial discrete state not only with the ionization continuum, but also with the Coulomb condensation of the energy terms of Rydberg atoms. Thus, in addition to ionization, we can have transitions in which the upper highly-excited states (HEA) become populated. The probability that the system X_2^* will survive on a covalent term prior to the onset of ionization is $P = 1 - p_m$ were p_m is the probability of transition to other discrete states X^{**} that are different from the initial state. These states in turn take part in associative and direct ionization processes

$$X^{**} + X \rightarrow X_2^+ + e, \tag{2.4}$$

$$X^{**} + X \rightarrow X^+ + X + e, \tag{2.5}$$

and also in the production of pairs of positive and negative ions, i.e.,

$$X^{**} + X \rightarrow X^+ + X^-. \tag{2.6}$$

The advent of laser methods was the beginning of extensive studies of ionization in binary collisions between Rydberg atoms:

$$X^{**} + X^{**} \rightarrow X_2^+ + e, \tag{2.7}$$

$$\rightarrow X^+ + X + e, \tag{2.8}$$

$$\rightarrow X^+ + X^-. \tag{2.9}$$

The high exchange cross section for a thermal collision between a metal atom (M) and a homonuclear (X_2) or heteronuclear (XY) diatomic halogen molecule was first noted in the 1930s. This large cross section (10^{-14}–10^{-15} cm^2) was interpreted at the time in terms of a model that was subsequently called the harpoon model. According to this, the reaction proceeds via intermediate states that are formed when an electron undergoes a transition from an alkali-metal atom to an electronegative molecule, and the theory retains the concept of covalent-term crossing for the reagents and band terms for the reaction products. However, in contrast to the cases considered above, we now have multidimensional potential energy surfaces, which complicates the associated quantum-mechanical calculations.

Chemi-ionization processes in atom-molecule collisions are usually multichannel phenomena:

$$\begin{aligned} M + XY &\rightarrow M^+ + XY^-, \\ &\rightarrow M^+ + X + Y^-, \\ &\rightarrow M^+ + X^- + Y. \end{aligned} \tag{2.10}$$

Molecular quantum chemistry employs the concepts of adiabatic and vertical electron affinities of molecules. The adiabatic affinity, which is analogous to the binding energy of a valence electron in an atom, corresponds to a transition between the ground vibrational states of the molecule and the corresponding negative ion. Vertical electron affinity implies transitions with the participation of vibrationally-excited states. According to the harpoon model, charged reaction products can originate in the dissociation or stabilization of an intermediate ionic complex. In simplified form, the total ionization cross section is given by

$$\sigma = 2\pi R_c^2 p'(1 - p'), \tag{2.11}$$

where p' is the average electron-transfer probability between the atom and the molecule for the mean impact parameter, the probability being calculated from the Landau–Zener theory. In the case of ground-state colliding particles in (2.10), the required energy is of the order of an electron volt.

The advent of laser technology has produced experimental data on rate of processes such as (2.10), which involve excited atoms and either release or absorption of energy.

The cross section for the production of an ion pair was found in Ref. 6 to depend on the degree of excitation of halogen-containing molecules colliding at thermal energies with alkali-metal atoms. The influence of vibrational excitation on the electron-transfer process may then be traced to a number of factors: a reduction in the reaction threshold energy, a change in the vertical electron affinity energy, and so on. These results are of undoubted practical interest for the detection of vibrationally-excited molecules. For halogen-containing molecules for which the slow-electron attachment rate constant is high (10^{-7} cm^{-3} s^{-1}, SF_6), the negative-ion yield of thermal collisions with HEAs is determined by the probability of attachment of a highly-excited electron (HEE). This follows from the theory and is confirmed by measurements of the ionization rate constants of HEAs with $n = 20 - 100$ in collisions with halogenide molecules. In the impulse approximation, the cross section for a collision between HEAs and a target molecule is determined by the cross section for the scattering of HHE with energies of the order of 0.001 eV by a halogen-containing molecule. Comparably high ionization cross sections (10^{-12}–10^{-13} cm^2) are observed in thermal collisions between HEA and H_2O, H_2, O_2, and other molecules when the rotational deexcitation of the molecule provides the energy necessary for the removal of the HHE.

There is now a sufficient number of published reviews (see, for example, Refs. 1–4 and 7) reporting reference material on the rates of reactions (2.1)–(2.10).

2.2. Fundamentals of the modern theory of chemi-ionization

The generally accepted theoretical description of chemi-ionization processes is based on the adiabatic approximation, as exemplified by Ref. 8, the basic ideas of which will be used here.

Penning associative ionization occurs when the excitation energy of an atom X* is greater than the ionization potential of the particle Y. For all nuclear separations, the molecule X*Y is then in an autoionizing state that decays with the emission of an electron and the formation of the molecular ion XY^+, provided this ion can exist. The corresponding potential curves are shown in Fig. 1a. The fundamentals of the theory of PAI are in developed in Refs. 9 and 10. If the excitation energy is lower than the ionization potential, there are two ways in which reaction (2.1) can proceed. In the first, the diabatic potential curves $U_\beta(R), U_i(R)$ of the quasimolecule X*Y and the molecular ion XY^+ approach one another, but do not cross. A transition due to the nonadiabatic coupling of electron and nuclear motions then takes place for a wide range of nuclear separations when the curves come close enough to one another. The corresponding potential energy curves are shown schematically in Fig. 1b. A theoretical analysis of the AI process with the potential energy curves illustrated in Fig. 1b can be found in Refs. 11–13. In the second possibility (Fig. 1c), the diabatic term $U_\beta(R)$ crosses the Coulomb states of X**Y and the continuum limit $U_i(R)$ near the nuclear separation $R=R_c$, and becomes an autoionizing state for $R \leqslant R_c$. The theory of AI based on this term scheme, but without interaction with the Coulomb condensation, was presented in Refs. 14 and 15. The AI reaction is basically a process with an infinite number of channels, which occurs with the participation of Rydberg and continuum states. In the 1970s, most theoretical studies of the AI process ignored the multitude of crossings that occur well before the limit of the molecular ionic continuum is crossed by the initial covalent term of the quasimolecule. On the other hand, attempts to allow for multiple term crossing (which is unavoidable for sufficiently high principal quantum numbers of the initial state) by the traditional approach, in which each crossing is considered separately, have not led to satisfactory results. A better approach seems to be to develop methods capable of dealing with multiple term crossing. One such method[16] is the "diffusional approach to impact ionization of excited atoms."

This phrase refers to diffusion over the energy states of the quasimolecule in a single collision event in which the basic collision parameter is the binding energy of the bound electron. The result of this "diffusion" is that, for $R \to \infty$, the initial single term of the quasimolecule transforms for $R \sim R_c$ into a braid with a conical cross section and effective width of the order of 1 eV (alkali-metal atoms) in the region in which the covalent and ionic terms are found to cross (Fig. 2).

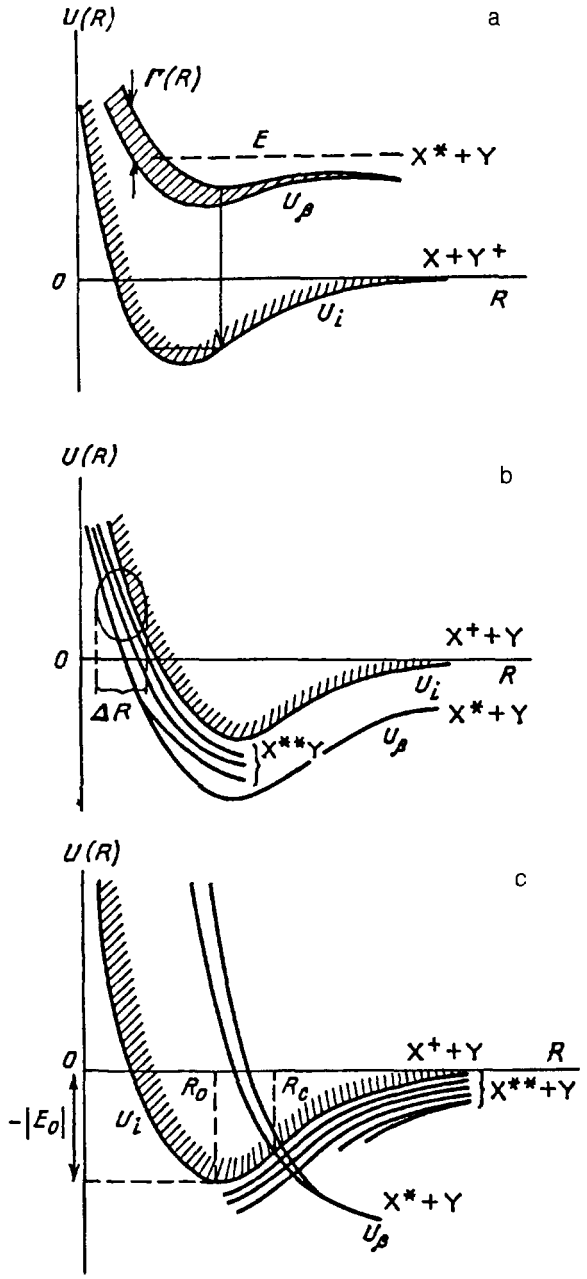

FIG. 1. Potential curves of the quasimolecule X*Y. E—total energy of the system, $\Gamma(R)$—width of a quasistationary state, X*Y, X**Y—diabatic Rydberg molecular states adjacent to the limit of the continuous spectrum $U_i(R)$, ΔR—transition region, $U_\beta(R)$—covalent diabatic term of the system X*Y; a—excitation energy of atom X* greater than the ionization potential of atom Y; b—excitation energy of atom X* smaller than the ionization potential of particle Y, diabatic potential curves of X*Y and X^+Y approach one another without actually crossing; c—same as b but with the crossing of the potential curves of the quasimolecule and molecular ion.

The theory of dissociative recombination (DR) of the slow electron and the molecular ion, with Rydberg levels taken into account, should correctly reproduce on the complex plane of the electron momentum the motion of the poles of the adiabatic S-matrix as a function of nuclear separation. The analytic structure of the S-matrix in the neighborhood of the continuous spectrum limit differs

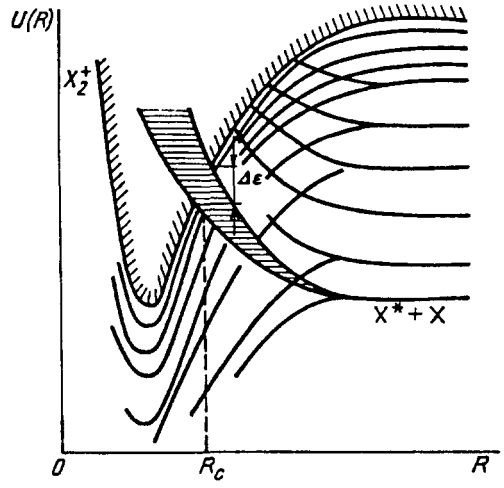

FIG. 2. Qualitative illustration of the crossing of covalent and ionic term crossing in the AI "diffusion" model.[16]

from its usual form (reproduced, for example, in Ref. 17) because of the presence of the long-range Coulomb field. The DR theory (cf. Refs. 18–20) shows that Rydberg states have a considerable effect on the DR cross section as a function of electron energy. Hence it is clear that the Coulomb condensation of the energy levels has to be taken into account in any valid calculation of the probability of the AI reaction that is the inverse of DR. A quantum theory[21] dealing with the motion of nuclei has now been developed in a practical form for the near-threshold endothermic AI in collisions between a weakly-excited atom X* and an atom Y. The theory takes account of the nonadiabatic interaction between Rydberg states and the ionization continuum. The entire analysis is based on the integral quantum defect method (QDM) using the potential energy curves of Fig. 1c.

The motion of a weakly-bound electron in a highly-excited state of a molecule can be looked upon as the motion of a particle in the Coulomb field that is perturbed by the scattering of the electron by the ion core. This is why the concepts and methods of the quantum theory of scattering of slow electrons by molecular ions can readily be used to examine processes involving a Rydberg electron. Indeed, this suggests that the multichannel quantum defect method could be useful in such calculations. The original formulation of the method for the case of diatomic molecules was given by Fano.[22,23] However, this approach relies on the selection of a set of solutions of Schrödinger's equation that satisfy particular boundary conditions, and suffers from the difficulty that the nonadiabatic rotational electron wave functions must then be joined to the adiabatic electron wave functions in the neighborhood of the ion core (in a state in which the quantization axis for the orbital angular momentum is the line joining the nuclei). It follows that QDM based on an integral representation of the Schrödinger equation is a more convenient approach[21,24–26] to the description of AI. The integral variant of QDM enables us to express the cross section for AI along different channels in terms of the scattering of HEE by a molecular ion and the adiabatic K-matrix that describes the mixing of electron states with different orbital angular momentum l.

The semiclassical theory of endothermic AI near the threshold was developed in Refs. 27 and 28, and the quantum mechanical variant of the theory is presented in Ref. 21. Several assumption were introduced in Ref. 21 in order to simplify the corresponding calculations: the orbital angular momentum l of the Rydberg electron was conserved and was not coupled to the angular momentum of relative motion of atoms X* and Y, and the main contribution to process (2.1) was due exclusively to states in the Rydberg series with ionization limit corresponding to the nearest closed channel. All the parameters used to calculate the partial AI cross sections are then adiabatic characteristics that can be calculated either by quantum-chemical methods or deduced from experimental data. However, the number of such parameters cannot be too high, since otherwise a large volume of *a priori* information would be necessary before one could calculate them for a particular pair of atoms. This limits the predictive power of the theory.

According to Ref. 21, the total cross section σ_{AI} is a linear function of energy near the threshold. This differs from the $E^{3/2}$ law obtained for endothermic AI in the semiclassical approximation.[28]

To illustrate the possibilities of the theory presented in Ref. 21 in relation to the analysis of experimental data, let us consider the following expression for the rate of AI in a gas whose temperature is much less than the energy of a vibrational quantum of the molecular ion X^+Y (it is assumed that the energy spread of the ensemble of particles is much smaller than the separation of the Rydberg levels in a closed channel):

$$k_{AI}(T)=AS(T)T^{1/2}\exp(-E_\beta/T), \tag{2.12}$$

where

$$A=8\pi^2R_0^2\left(\frac{2}{\pi M}\right)^{1/2},$$

$$S(T)=\sum_\beta g_\beta V_\beta^2\left(\alpha_{\beta 0}^2+\alpha_{\beta 1}^2\frac{\gamma_i}{T\gamma}\sum_{\nu>\bar\nu}^{\infty}\frac{\exp(-\varepsilon_\nu/T)}{\nu^3}\right),$$

g_β is the statistical weight of the dissociative reaction channel, ε_ν is the position of the Rydberg resonance relative to the reaction threshold, M is the reduced mass of X* and Y, $\alpha_{\beta\nu}$ is the Franck–Condon factor for the transition between the associative $[U_{(\beta)}]$ and the ionic $[U_i(\nu=0,1)]$ terms, $2V_\beta^2=\Gamma_\beta$ is the adiabatic autoionization width of the dissociative term, γ_i is the autoionization rate, $\gamma=\gamma_i++V_\beta^2$ is the nuclear separation that corresponds to the crossing of the initial and final (ionic) potential energy curves of the quasimolecule, E_β is the AI reaction threshold in the center of mass system of the βth channel, $\bar\nu=(2\omega_e)^{-1/2}$, and ω_e is the frequency of a vibrational energy quantum in the molecular ion.

At low temperatures $T\leqslant(\bar\nu)^{-3}$, the Rydberg resonances can depend appreciably on the temperature func-

tion $S(T)$, but for $T \ll E_\beta$ this occurs in the region where $k_{AI}(T)$ is exponentially small. The exception is the case $E_\beta \leqslant T \ll \omega_e$ when $k_{AI}(T)$ is of the order of $T^{-1/2}\exp[-(E_\beta+\varepsilon_{\bar{v}})/T]$. When $\omega_e \gg T \gg (\bar{v})^{-3}$, the function $S(T)$ becomes equal to a constant, and the presence of Rydberg resonances affects only its magnitude. When $T \geqslant \omega_e$, the rate constant is given by

$$k_{AI}(T)=A\left(1+\frac{2T}{E_\beta}\right)T^{1/2}\exp\frac{T}{E_\beta}, \tag{2.13}$$

where

$$A=\left(\frac{8}{\pi M}\right)^{1/2}\omega_e^{-1}\sigma_{AI}(\omega_e)E_\beta.$$

The reaction $N(^2D)+O(^3P)\rightarrow NO^+(X'\Sigma^+)+e$ has been used to test the above theory. Calculations have shown that (2.12) and (2.13) yield the AI reaction rate to within 15% at temperatures in the range 4500–7500 K. The resulting temperature dependence is in agreement with experimental data.

The adiabatic approximation is physically valid for associative ionization in collisions between weakly excited and ground-state atoms. However, the adiabatic approximation breaks down when the AI process involves a highly excited Rydberg atom, and a fundamentally different AI mechanism comes into play.

When a Rydberg atom $X^{**}(n)$ collides with a particle Y, this particle can fly past the atomic residue X^+ with impact parameter p that is small in comparison with the radius $r_n \sim n^2$ of the Bohr orbit of an outer electron of the atom $X^{**}(n)$. Associative ionization then occurs as a result of energy exchange between the outer electron and the inner electrons of the quasimolecular or molecular ion.

The energy exchange mechanism can become particularly effective in the case of the homonuclear system $(X^+,X)+e$ in which the resonant charge transfer process in the quasimolecular ion X^+Y proceeds with a high cross section.[29,30] AI in the collision between $X^{**}(n)$ and the corresponding atom X or a totally different atom Y is discussed in the spirit of perturbation theory in Refs. 3 and 4 in resonant and quasiresonant cases. Analysis of the results obtained there shows that the transition probability can reach values of the order of unity for intermediate values of n ($n \approx 10$–15 for alkali metal atoms), and the validity of perturbation theory becomes problematic. For $n<10$, the theory given in Refs. 14 and 31 provides a sufficiently accurate description of experimental data, although it seems reasonable to use approaches based on the adiabatic approximation in this range of values of n. It is clear from the foregoing that that theory of AI for collisions involving Rydberg atoms will need further attention in the future.

An interesting step in this direction was undertaken in Ref. 32 which examines the AI reaction due to the interaction with the dipole moment of the quasimolecular (molecular) ion X^+Y in the collision between an atom Y and an atomic residue X^+. The dipole moment of the ion X^+Y is due to the change in the position of its inner electrons relative to the nuclei of X^+ and Y during the collision. In this mechanism, there is no change in the electronic state of the ion X^+Y, so that AI proceeds by energy transfer between the Rydberg electron and the relative motion of the atoms. It is shown in Ref. 32 that this mechanism reaches its maximum efficiency for the system X+Y when the potential energy U_i has a deep well E_0 and the frequency ω_e of the lowest vibrational quantum of the ion X^+Y is high. These conditions are well satisfied, for example, in the collision between a highly excited hydrogen atom and inert-gas atoms.

Perturbation theory is used in Ref. 32 to show that transitions of the Rydberg electron occur with maximum probability when the transition frequency is $\omega_{n\varepsilon}=|\varepsilon_n|+\varepsilon$ where $|\varepsilon_n|=(2n^2)^{-1}$ and ε is the energy of the free electron, which is lower than or of the order of ω_e. The AI probability falls exponentially when $\omega_{n\varepsilon}>\omega_e$ and $E \ll E_0$. It is therefore interesting for the physics of low-temperature plasmas to consider the AI reaction in which the molecular ions X^+Y are produced only near the dissociation limit (E,ε are measured from the dissociation limit of X^+Y). The efficiency of the AI mechanism proposed in Ref. 32 has been tested in the case of a hydrogen HEA colliding with a helium atom. Calculations suggest that this mechanism predominates for $n<25$–30 and $T \approx 300$ K over ionization (calculated from the model assuming the elastic scattering of a weakly bound electron by the incident atom[33]). Up to now, questions relating to the theory of ionization in collisions between two Rydberg atoms have be investigated to a lesser extent. The Monte Carlo calculations of the cross sections for this process have therefore retained their value. The cross section given in Ref. 34 is (in atomic units)

$$\sigma(n,v)=0.703v^{-0.65}n^{3.35} \tag{2.14}$$

and was used in Ref. 35 for $v/v_e \ll 1$ to calculate the chemiionization rate constants (2.7) and (2.8) for lithium (v_e is the orbital velocity of a Rydberg electron and the cross section has a maximum for n for which the velocity of a highly-excited electron becomes equal to the atomic velocity). The function $k_{AI}(n)$ calculated in the temperature range 1–1000 K has at thermal energies the characteristic structure shown in Fig. 3. This is due to quasiresonances between twice the excitation energy of the initial state and the excited ionic complex $X^*(n)X^+$. We note the inverse character of the function $k(T)$ in different exit channels, i.e., associative and Penning ionization. It also follows from this model that the branching ratios of the chemiionization reactions (2.7) and (2.8), $\gamma=k_{AI}/k_{PI}$, vary between 5% and 40% in the temperature range 1000 – 10 K.

In thermal and subthermal collisions, the covalent configuration $X^{**}X^{**}$ is stable against ionization for large nuclear separations, but may split into an ion and an atom in an excited state. Moreover, binary collisions can take Rydberg atoms to excited states that are different from the initial excited states, since the primary quasimolecular terms are coupled by a nonadiabatic interaction to covalent terms corresponding to other close-lying stable atomic configurations.

For an initial $nPnP$ configuration of alkali-metal ions, this can be the configurations $nSnS$, $nS(n-2)D$, and so

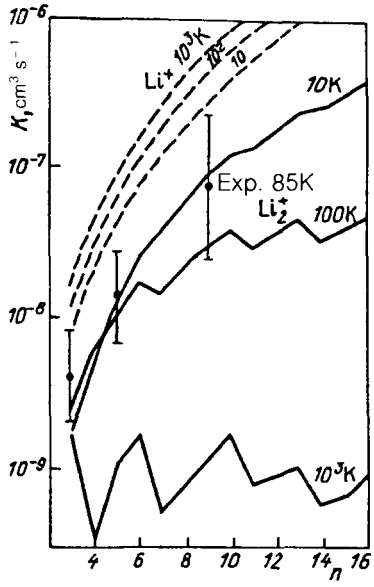

FIG. 3. Chemi-ionization rate constant of binary collisions between Rydberg atoms; dashed line—calculated using Ref. 34 for process (2.8), solid curve—calculated[35] for (2.7), points—measured values[35] ($T=85$ K).

on. The alkali-metal atoms are known to have excited states of the negative ion with excitation energy comparable to twice the energy of the excited Rydberg atom. As the ions X^+ and $(X^*)^-$ come closer to each other, the ionic autoionizing terms can also interact with neighboring covalent configurations. The open channels enumerated above ensure that interactions occurring in slow collisions between two Rydberg atoms can populate low-lying atomic configurations and produce negative and positive ions in different autoionizing states, e.g., with the production of the $X^+ + X^*$ pair in the exit channel (Fig. 4).

It is often useful to estimate the ionization rate constant without analyzing in detail the dynamics of possible transitions between configurations, using the expressions

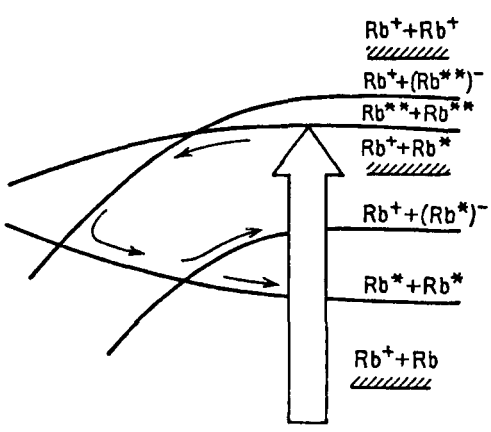

FIG. 4. Schematic illustration of term quasicrossing for the collision of two highly excited rubidium atoms.

obtained in the classical approximation[36] (see also Refs. 2, 37, and 38) for the PI process due to the dipole-dipole interaction.

The model of Refs. 36–38 was extended in subsequent publications by taking into account the influence of the structure of quasimolecular terms and the exchange interaction on the autoionization width $\Gamma(R)$, i.e., the ionization probability per unit time for given atomic separation R. The model has been tested in calculations of the cross section for Penning ionization in thermal collisions with the participation of excited and ground-state inert-gas atoms and also Cd, Zn, and Hg atoms (see Ref 41).

According to Ref. 2, the probability of reaction (2.8) per unit time for given nuclear separation can be written in the form

$$W(R)=2\pi|V_{\rm if}(R)|^2 g_{\rm f}, \tag{2.15}$$

where subscripts i and f refer to the states of the quasimolecules $X^*(nL)$, $X^*(nL)$ and $X(n'L')$,X^+; $V_{\rm if}$ is the matrix element between the initial (i) and final (f) states of the dipole-dipole interaction operator between the atoms and $g_{\rm f}$ is the density of final states.

To calculate the mean transition probability to all allowed final states, we have to average in (2.15) over the initial states and then sum over the final states. The Penning ionization cross section $\sigma_{\rm PI}$ can then be expressed in terms of the photoionization cross section $\sigma_{\rm ph}$ of the excited atom $X(nL)$ in its initial state. Using the Kramers approximation for the cross section $\sigma_{\rm ph}$, and assuming that the path of the atoms is rectilinear, we have

$$\sigma_{\rm PI}(v)=\frac{11.9}{v^{2/5}(n^*_{\rm eff})^2}\left(\sum_{\rm f}\frac{f_{\rm fi}}{\omega_{\rm if}}\right)^{2/5}, \tag{2.16}$$

where v is the relative velocity of the atoms, $n^*_{\rm eff}$ is the effective principal quantum number of the initial excited state of the atom $X^*(nL)$, $f_{\rm fi}$ is the oscillator strength for transitions of the atom from low-lying states among final (f) states and the initial (i) excited state of the atom, $\omega_{\rm if}$ is the corresponding transition frequency, and the sum is evaluated over all the possible final states $n'L'$.

We note that (2.16) is valid only for impact parameters greater than the sum of the Bohr radii of the two highly excited atoms ($\rho \geqslant 4\pi^{*2}_{\rm eff}$). It is only in this case that we can use the multipole expansion for the electrostatic interaction. At the same time, the range $\rho \leqslant 4\pi^{*2}_{\rm eff}$ can provide appreciable contribution to ionization. Hence, to obtain a reliable estimate for σ on the basis of Refs. 2 and 36–38 we must calculate the total autionization probability for the decay of the quasimolecule $X^{**}X^{**}$ for nuclear separations $R < 4\pi^{*2}_{\rm eff}$, which is a problem in its own right. Moreover, a selective population of low-lying states, giving rise to the corresponding features in the fluorescence and electron spectra, may be expected in such experiments. This type of calculation was performed in Ref. 42 for the initial 11^2P state of the rubidium atom. It showed that the greatest contribution to ionization is provided by channels with the production of Rb^+ and rubidium atoms in the 9^2S and 7^2D states whose thresholds lie closer to the 11^2P, 11^2P configuration than to any other. The channel produc-

ing of the 9^2S states is then found to provide the largest contribution since the energy difference between the 11^2P, 11^2P and Rb^+, $Rb9^2S$ configurations is of the order of 50 cm^{-1}. However, the validity of the theoretical model from Refs. 36–38 in the case of such closely lying atomic configurations appears to require special examination. Reaction channels producing atoms in any of the other energetically possible excited ^2S and ^2D states are less effective by an order of magnitude, whereas those producing atoms in the ground state are less effective by two orders of magnitude.

The electron spectra from reactions (2.1)–(2.9) are an important source of information on the structure of quasimolecular terms, and provide a basis for the reliable identification of such terms. The basic principles for the determination of these spectra in the classical approximation are discussed in Ref. 2 for the repulsive part of the interaction potentials. It is shown in Ref. 41 that at energies below the maximum energies at which the orbiting effect is possible, the electron spectrum displays two types of feature, namely, statistical, determined by the dependence of the emitted electron on the nuclear separations, and dynamic, due to the motion of the atoms in the initial attractive potential.

In the subthermal energy range there can be new quantum-mechanical atom-molecule interaction effects as the de Broglie wavelength of the system of colliding particles becomes greater than the typical separation between the interacting particles. Quasiclassical ideas then cease to be valid, and the resulting new phenomena can only be discussed in terms of wave-mechanical ideas and involve effects such as interference between incident and scattered partial waves. In the usual thermal energy range, such interference effects are reduced because an average is taken over a large number of partial waves, i.e., the effective number of partial waves in the de Broglie wave expansion is smaller in the subthermal range. Studies in the subthermal range provide us with a way of obtaining new quantitative information on the particle interaction potential and the structure of quasimolecular terms.

At low velocities, there is also a significant increase in the particle collision time. This in turn means that weak long-range interactions such as the magnetic dipole-dipole interaction begin to provide an increasing contribution, so that particles can be "captured" into quasistable orbitals and intermediate states can be formed. Such conditions are typical of essentially nonisotropic scattering effects, e.g., a halo with a complex oscillatory structure. This structure can also be investigated only for a finite number of partial waves. Finally, the probability of radiative and spontaneous transitions in subthermal collisions can be close to unity, and radiation is an effective factor in collision dynamics even in relatively weak light fields. This offers us the possibility of new experiments with radiation-induced collisions.

3. CHARACTERISTICS OF AN ENSEMBLE OF EXCITED PARTICLES IN CHEMI-IONIZATION EXPERIMENTS AND THEIR INFLUENCE ON IONIZATION KINETICS

Selective population of individual excited states of atoms and molecules by optical excitation is an independent method in experimental physics, widely used in chemi-ionization studies. The idea that optical excitation of a gaseous medium could be used to stimulate chemical reactions was first implemented[45] as far back as the 1920s. Subsequent advances in the application of the method had to await the advent of the tuneable laser and its applications. We shall not consider in this review the polarization effects in the interaction between light and matter and in the alignment and orientation of atoms. This approach is justified in optically dense media in which these effects are relatively insignificant,[46] e.g., in low-temperature plasmas. When this assumption is adopted, the radiation field is described by the intensity I_ν or the energy flux $h\nu I_\nu$. Absorption of light can then be characterized by the spectral absorption coefficient $\varkappa_\nu$. Whatever the absorption-line profile, the integral absorption coefficient is given by the universal expression

$$\int_0^\infty d\nu \varkappa_\nu = \bar{\sigma} A N_0, \quad \bar{\sigma} = \frac{\lambda^2 g^*}{8\pi g_0}. \tag{3.1}$$

This expression enables us to relate the integral absorption coefficient to the optical transition probability A (a fundamental concept in the theory of radiation) in terms of the optical transition wavelength λ, the statistical weights g^* and g_0 of energy levels, and the concentration N_0 of ground-state atoms. In the special case of incident light with $I_\nu = \text{const}$ within the characteristic width $\Delta\nu$ of an absorption line, the probability of excitation of an atom is given by $W_{\text{exc}} = I_\nu A \bar{\sigma} d^2\omega$ where $d^2\omega$ is a solid angle element. The quantity $F = I_\nu \Delta\nu d^2\omega$ is the flux of photons within the spectral line width $\Delta\nu$. Hence

$$W_{\text{exc}} = \sigma_\nu F,$$

$$\sigma_\nu = \bar{\sigma} \frac{A}{\Delta\nu} = 0.027 \frac{f}{\Delta\nu}. \tag{3.2}$$

The numerical coefficient in this expression was obtained by substituting numerical values for the constants c, m, e and f is the transition oscillator strength. For elements with intermediate atomic weight and temperature of atoms in the range 100–1000 K, the light absorption cross section σ_ν (cross section for the optical excitation of the atom) is found to be of the order of 10^{-12} cm^2 ($\nu \approx 10^8$ MHz).

The energy and spatial distribution density $N^*(x,v)$ of excited atoms is a fundamental characteristic of an excited gaseous medium. The evolution of N^* depends significantly on the ratio of radiative and radiationless channels for the decay (quenching) of excited states. Let us introduce the effective probability of radiative decay to the ground state: $A_{\text{eff}} = M_{\text{eff}} A$, where M_{eff} represents the trapping of resonant radiation. Consider the following two cases:

(a) *Externally incident photon is absorbed once (single scattering regime).* All the characteristics of the gaseous

medium are determined by the individual absorption of the primary photon, localized at a particular point. The radiating atoms do not migrate as a result of radiation transfer (trapping).

(b) *Multiple scattering*. This occurs in optically dense media, $\varkappa_0 l \gg 1$, where $\varkappa_0$ is the absorption coefficient at the central frequency of the line ($\nu=\nu_0$) and l is a typical linear dimension of the absorbing medium. When $A_{\text{eff}} \gg W$ where W is the probability of quenching in any radiative or collisional deactivation channel other than the resonance channel, the distribution $N^*(x,v)$ evolves by multiple scattering of light photons throughout the scattering medium. In both cases, the primary excitation density $\alpha^*(x,v)$, i.e., the so-called primary excitation source function, depends on both the spectral composition of the incident radiation and on its direction of propagation Ω at the point x. For single scattering (short-lived excited atoms), the functions $N^*(v)$ and $\alpha^*(v)$ at the point x are related by a Boltzmann-type transport equation which does not explicitly depend on the coordinate x, since the atom does not significantly change its position during its lifetime $(A+W)^{-1}$. When atoms are excited by a source with a wide spectral composition, e.g., a dye laser, we have a highly directional beam with intensity $I_\nu=I_0=\text{const}$ and frequency spread $|\nu-\nu_0|$.

An important characteristic of optical excitation is the integral strength of primary excitation sources $\alpha^*=\int d^3x\alpha^*(x)$. The velocity distribution of the primary sources of excitation for $\varkappa_0^{\text{D}} l \gg 1$ (D refers to the Doppler line profile) differs significantly from the equilibrium (Maxwell) distribution.

The effect of line structure on the absorption of radiation is of practical interest for the transformation of the energy of the source of excitation into the excitation energy of the medium, and the light-absorption diagnostics of a medium. Line structure (e.g., multiplet structure) ensures that absorption against a line background or absorption against a continuous background are different as compared with the case of a single unsplit line.

Thus, for spectrally nonoverlapping components of a multiplet with a Doppler profile, the splitting of the bottom level into n sublevels increases by the same factor the absorption in a continuous background, independently of the ratio of statistical weights $g_i[\ln(\varkappa_0 l \gg 1)]$. Conversely, for a Lorentz profile, the increase in absorption due to the line structure does depend on the ratio of the statistical weights g_i and reaches its maximum value of $n^{1/2}$ for $g_1=g_2=g_3\ldots\ldots=g_n$. The reverse situation is observed for absorption on a line background.

The above discussion was based on the assumption of thermal motion of ground-state and excited-state atoms with an isotropic velocity distribution function. Low-temperature plasma is a model of this type of medium. However, at present, the attention of researchers is increasingly drawn to atomic beams (AB). The collisionless, monodirectional stream of particles in the AB is a convenient and universal source for a wide range of fundamental and applied problems.

The theoretical analysis of questions relating to the absorption and emission of light by ABs is more complicated than for a gas-filled cell. This is due, in the first instance, to the particular velocity distribution of the beam particles.

When the perfect AB with no velocity components in the x and y directions ($v_x=v_y=0$, $v_z\neq 0$) and no collisions in the beam, is crossed with a monochromatic beam of radiation of frequency ν, popagating at an angle θ to the z axis (along which the beam is travelling), there is a unique relation between the frequency of the incident light and the component of the velocity of an atom along the light beam. This gives rise to the selective excitation of the ensemble of atoms with the fixed velocity $v_z=v$, where $v=c(\nu-\nu_0)/\nu_0 \cos\theta$. When the natural line width is taken into account, v_z is found to be distributed around v with a narrow distribution width $\Delta v \sim Ac(\nu_0 \cos\theta)^{-1}$. When $\theta=\pi/2$, the v_z distribution of optically excited atoms is the same as the distribution of ground-state atoms, and there is no Doppler velocity selection. Absorption of light is then due to the natural line profile, i.e., the narrow frequency range of the order of the natural line width that contains the line center. In a practical beam, the transverse velocity components v_x, v_y are not zero and it is useful to formulate the restrictions on the AB model parameters, so that these parameters can be calculated in the practical situation in which the atomic beam is crossed with a beam of light.

It may be assumed that the exit aperture of the source is effectively a point. This ensures that the velocity distribution in the AB has a simple analytic form. The same restriction may therefore be formulated by saying that the solid angle subtended by the excitation region at the source is small in comparison with the solid angle $\pi\beta^2$ where β is the angle of the conical beam into which the particles are emitted by the source. It follows that the excitation region must be at a large distance from the source. This assumption, and the assumption that the dimensions of the excitation region are small in comparison with the distance to the source exit, together allow us to consider that the geometric parameters of the beam in the excitation region are independent of the coordinate z along the beam axis, and that the beam geometry in the excitation region can be approximately represented by a cylinder. Finally, the beam aperture angle β is assumed small, so that we need only take into account terms of the order of β^n where $n \leqslant 2$.

The relationships obtained under these assumptions, which enable us to determine the density distribution of the primary sources of excitation are reproduced in Ref. 46.

In the classical optical excitation scheme, the absorbing medium is illuminated in a given direction. This gives rise to practical difficulties whenever it is desired to produce a large volume of a uniformly excited medium, since one is then forced to use relatively low densities of ground-state atoms and therefore low densities of excited atoms. On the other hand, optical excitation by a laser beam ensures—at least in principle—that a high degree of excitation with the saturation of the optical transition is produced within the confines of the laser beam. A convenient method is described in Ref. 46 for the excitation of an absorbing medium. It produces a uniform distribution of

excitation, $N^*(x)=\text{const}$, under isotropic illumination of the absorbing region with wide-spectrum light under radiative transfer conditions.

In the latter case, the excited-particle concentration in the expression for the chemi-ionization rate is reliably determined by traditional optical diagnostics, using the absorption method, and the relative-velocity distribution of the excited particles is found to be Maxwellian. A similar excitation technique was used in the very first series of studies of AI of resonantly-excited alkali-metal atoms.[46] When the absorbing medium is excited by a beam of light in a particular direction, we again find that the distribution function has a simple analytic form. This is the case of axisymmetric excitation by a beam of light along the axis of a cylindrical configuration.[47] The AI studies reported in Refs. 48 and 49 employed a cylindrical laser beam and a plane-parallel layer of a vapor. The problem of finding $N^*(x)$ then reduces to the solution of the Biebermann–Holstein integral equation.

Recent experimental determinations of the chemi-ionization rate in collisions of resonantly excited atoms employ a method[50] that relies on measurements of the concentration of absorbing (ground-state) atoms. The method is based on the measurement of the ratio of the effective lifetime τ to the radiative lifetime τ, due to radiation trapping. This can be used to determine the concentration of absorbing atoms if its dependence on the optical density $k_0 l$ is known *a priori* (l is a typical linear dimension of the vapor-containing cell). The expression obtained in the simplified Milne theory of radiation transfer was used in Ref. 50 for τ_{eff}/τ. It is important to note that the application of the Milne theory involves a fit of the theoretical result to the experimental data through the use of the effective size l_{eff} of the reaction zone. We also note that, in contrast to the case of the gas-filled cell for which Milne's theory is valid when $1\leqslant\tau_{\text{eff}}/\tau\leqslant 20$, this region shrinks to $1\leqslant\tau_{\text{eff}}/\tau\leqslant 5.5$ for a collimated AB. Calculations of radiation trapping effects in different types of atomic beam are described in Refs. 51–53. Analysis of the experiments reported in Ref. 54, which employed two crossed beams and used the method developed in Ref. 53 to calculate τ_{eff}, has shown that the authors of Ref. 54, who relied on the unmodified Milne theory of radiation transfer to calculate the concentration of absorbing atoms, may have underestimated it by a factor of 2.1 (Ref. 55).

Optical excitation of an atomic (molecular) beam was noted in Ref. 56 as a promising method of investigating collisions between excited atoms in the beam itself. This is recommended in the first instance as a means of studying binary collisions between atoms in short-lived excited states. The production of charged particles in AI-type reactions during the excitation of resonant atomic levels is of particular interest for applied physics. Such reactions constitute an efficient way of ionizing a medium by exposure to light quanta with energies below the ionization energy of an isolated atom. This principle is exploited in 'resonance ionization spectroscopy' with numerous modern applications.[3]

The solution of this problem must begin with an analysis of the effect of the atomic velocity distribution on the kinetics of the elementary process, which we shall base here on the research reviewed in Ref. 55.

When elementary collision processes involving neutral components of plasmas are described, it is usual to assume that the particle velocity distribution is isotropic. The gas-filled cell, widely used in studies of elementary processes, is an analog of this situation. The relative velocity distribution of identical colliding particles is well known for this situation. Atomic and gas-dynamic beams are increasingly used in research and are expected to find still more extensive applications in conjunction with the technology employed in laser chemistry and physics. The atomic beam (AB) is also an important, and widely used, tool in atomic spectroscopy.

Consider a perfectly collimated atomic beam. In state of the art equipment, the velocity component of the beam particles at right angles to the beam axis (this component determines the beam divergence) does not exceed a few percent and has little effect on the collision rate. We shall take the velocity distribution of ground-state atoms in effusive or gas-dynamic atomic beams in the common form

$$f(v)=\frac{v}{\Gamma_1}\exp\left[-\frac{(v-u)^2}{v_0^2}\right],\qquad v\geqslant 0,\quad v_0=\left(\frac{kT_{\text{es}}}{\mu}\right)^{1/2}, \tag{3.3}$$

where v_0 is the characteristic thermal velocity, determined by the thermal motion of the beam particles, u is the mass velocity of the gas, and Γ_1 is a normalizing constant that can be found from the condition

$$\int_0^\infty f(v)\mathrm{d}v=1.$$

For a gas-dynamic beam, the quantities u and T_{es} are determined by physical processes in the beam source. For an effusive source (ES), the mass velocity is $u=0$ and the temperature T_{es} represents the temperature of the gas in the effusive source.

Consider the evolution of the velocity distribution $f^*(v)$ of excited atoms in an atomic beam. We shall suppose that the beam particles are excited by electron impact or optically. In the former case, the velocity of a beam atom is much smaller than the velocity of an incident electron, and is unaffected by the electron impact, whereas optical excitation occurs at the central frequency of the atomic transition and the optical thickness of the beam is small. In the excitation region, the function $f^*(v)$ is then given by the expression

$$f^*(v)\sim v^2\exp\left[-\frac{(v-u)^2}{v_0^2}\right]\left[1-\exp\left(-\frac{l}{v\tau}\right)\right], \tag{3.4}$$

where l is the distance in this region and τ is the lifetime of the excited atom.

From the practical point of view, there is particular interest in the following two cases:

(1) The size of the excitation region, which is determined by the diameter or the electron or light beam, is appreciably greater than the characteristic path length $\bar{v}\tau$ for the deactivation of an excited particle ($\bar{v}$ is the mean velocity of beam particles). We then have $1-\exp(-l/v\tau)\approx 1$ and $f^*(v)$ becomes identical with $f(v)$. This situation is typical for the excitation slow short-lived atoms.

(2) $l \ll \bar{v}\tau$. Here $1-(-l/v\tau)\approx l/v\tau$ and the distribution of excited atoms differs significantly from (3.3). This situation occurs for high mass velocities in gas-dynamic beams or during the excitation of long-lived (metastable) atoms in effusive atomic beams.

The expression given by (3.4) can be written for both cases in the combined form

$$f^{\lambda}=\frac{v^{3-\lambda}}{\Gamma_{\lambda}}\exp\left[-\frac{(v-u)^2}{v_0^2}\right], \quad v\geqslant 0, \tag{3.5}$$

where $\lambda=1$ corresponds to case (1) and $\lambda=2$ to case (2); Γ_{λ} is a normalizing constant that can be found from the condition

$$\int_0^{\infty} f^{\lambda}(v)\mathrm{d}v=1.$$

In the case of excitation by electron impact under the conditions similar to those prevailing in gas-discharge plasmas, the velocity distributions of excited and ground-state atoms are identical. To calculate the rate constants for the collision process, we have to know the relative-velocity distribution function $F(v_{\mathrm{col}})$ of the colliding atoms, where $v_{\mathrm{col}}=|\mathbf{v}_1-\mathbf{v}_2|$ and $\mathbf{v}_1$, $\mathbf{v}_2$ are the velocities of the colliding particles.

3.1. Collisions within a single beam

In this case

$$F^*(v_{\mathrm{col}})=\int_0^{\infty} f^{\lambda_1}(v_1)\mathrm{d}v_1 \times \int_0^{\infty} f^{\lambda_2}(v_2)\mathrm{d}v_2\delta(v_{\mathrm{col}}-|\mathbf{v}_1-\mathbf{v}_2|), \tag{3.6}$$

where $f^{\lambda_1}(v_1), f^{\lambda_2}(v_2)$ are the velocity distribution functions of the colliding particles and δ is the Dirac delta-function. There are three possible cases, depending on the type of colliding particles and the mass velocity of the beam:

1. $F^{*1;1}$: $\lambda_1=\lambda_2=0$, which corresponds to collisions between short-lived excited atoms with each other or with ground-state atoms.

2. $F^{*1;2}$: $\lambda_1=1$, $\lambda_2=2$ or $\lambda_1=2$, $\lambda_2=1$. An example of this distribution function is provided by collisions between metastable and ground-state atoms in an atomic beam from an effusive source.

3. $F^{*2,2}$: $\lambda_1=\lambda_2=2$ describes the relative-velocity distribution function of two metastable atoms in an atomic beam from an effusive source or two short-lived excited atoms in a beam from a gas-dynamic source.

The expressions for $F^{*1;1}(v_{\mathrm{col}})$ and $F^{*1;2}(v_{\mathrm{col}})$ are given in Ref. 57. They depend significantly on the ratio of the mass velocity u to the characteristic thermal velocity v_0 of the particles. We shall confine our attention to two special cases that are of practical interest in physics: (1) $u\gg v_0$ and (2) $u=0$. The former condition is usually well satisfied for the gas-dynamic beam, and the distribution function then assumes the much simpler form (which does not depend on the type of colliding atoms):

$$F^*_{\mathrm{gd}}(v_{\mathrm{col}})=\sqrt{\frac{3}{\pi}}\,\frac{1}{v_0}\exp\left(-\frac{v_{\mathrm{col}}^3}{2v_0^2}\right). \tag{3.7}$$

The second case ($u=0$) corresponds to collisions within the atomic beam. In contrast to the gas-dynamic case, the functions $f^{*i;j}$ in effusive beams are different for different collision partners. The function $F^{*1,2}(v_{\mathrm{col}})$ has the simplest form:

$$F^{*1;2}(v_{\mathrm{col}})=\frac{2}{\sqrt{\pi}}\,\frac{1}{v_0}\exp\left(-\frac{v_{\mathrm{col}}^2}{2v_0^2}\right). \tag{3.8}$$

The functions $F^{*1;1}$ and $F^{*1;2}$ for an effusive beam are a more complicated.

3.2. Collisions in crossed atomic beams

Consider two identical perpendicular effusive atomic beams whose respective sources are at the same temperature. The relative velocity of particles with velocities v_1 and v_2 in the two beams is $v_{\mathrm{col}}=(v_1^2+v_2^2)^{1/2}$. Depending on the type of colliding particles, we again have three distribution functions:

$$F^{*i;j}(v_{\mathrm{col}})=\frac{2}{\Gamma\left(\frac{7-a}{2}\right)}\,\frac{v_{\mathrm{col}}^{6-a}}{v_0^{7-a}}\exp\left(-\frac{v_{\mathrm{col}}^2}{v_0^2}\right), \tag{3.9}$$

where $a=i+j-1$ and $\Gamma(x)$ is the is the Euler gamma-function. The value $a=1$ refers to collisions between short-lived atoms with one another or with ground state atoms; $a=2$ corresponds to collisions of metastable atoms with short-lived or ground-state atoms, and $a=3$ refers to collisions between metastable atoms.

The physical significance of 'freezing' of particles in an atomic beam can be seen from the following simple considerations. An effusive atomic beam is a beam of particles with monodirectional velocities. Only overtaking collisions are possible in this system, and the relative velocity (the difference between the speeds of the particles) is always less than the velocity of one of the colliding atoms. In low-temperature plasmas, the velocities of colliding atoms can have any direction, so that there are both overtaking and head-on collisions. The relative velocity can then exceed the velocity of an individual particle. A similar situation obtains in the gas-dynamic beam in which all the particle velocities again point in the same direction but the velocity component $v'=v-u$ is randomly distributed because the mass velocity u adds to the particle velocity. It follows that v' can be either positive or negative, so that both overtaking and head-on collisions are possible in a frame moving with velocity u. The greater the mass velocity u, the less stringent the restrictions imposed on the magnitude of the relative velocity in head-on collisions.

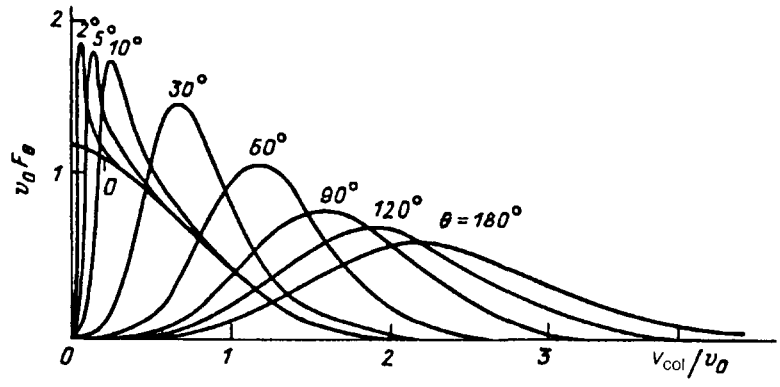

FIG. 5. Relative-velocity distribution function for thermal beams of particles crossing at an angle θ (Ref. 58). Values of θ in degrees are shown against the curves.

Advances in experimental chemi-ionization studies have led to a peculiar paradox whereby traditional techniques for the processing and comparison of experimental data have ceased to keep up with the new experimental techniques now available. In particular, published AI rate constants must now be corrected for errors introduced in determinations of concentration by optical methods under the conditions of resonant radiation trapping.[55] Inadequate allowance for trapping effects leads to significant errors in the concentration of excited atoms and, hence, to errors in the reaction rates. Another possible source of error in the interpretation of data is the polarization effect that is absent for ordinary (nonlaser) radiation sources. It was found in 1982 that the yield of molecular sodium ions from reaction (2.2) was a maximum when the polarization vector of the exciting radiation was parallel to the direction of the atomic beam. Studies of the polarization dependence of chemi-ionization rate constants yield more precise information on the nature of the quasimolecular autoionization terms of X_2^*. However, it is important to note that the probability of depolarizing collisions is usually ignored in this type of analysis. At the same time, we know that the corresponding cross sections are of the order of 10^{-14} cm^2 and can already be significant for particle densities $N_0 = 10^{10}$ cm^{-3}, i.e., in the practical beam experiment.

A single atomic beam may be looked upon as a special case of two crossed beams. An expression for the relative-velocity distribution function $F_\theta(v_{col})$ of atoms in two different thermal-particle beams at an arbitrary angle θ to one another ($0 \leqslant \theta \leqslant 180°$) is derived in Ref. 58. The distribution function for two beams containing particles of different mass and crossing at an angle of $\pi/2$ is given in Ref. 59. Graphs of $F_\theta(v_{col})$ are shown in Fig. 5. It is clear that, as θ increases, the curves spread into the high velocity region. In most beam experiments, the collimation angle is of the order of 10°, so that a rapid variation in $F_\theta(v_{col})$ when $\theta \leqslant 10°$ may, in a real experiment, affect significantly the reaction yield at low velocities v_{col}.

Analysis of differences between the distribution functions $F(v_{col})$ of the atomic beam and the gas cell (plasma) shows that, at high velocities, the behavior of theses functions is determined by an exponential factor whose argument for $F_{pl}(v_{col})$ is smaller by a factor of 2 than for $F_\theta(v_{col})$ when $\pi/2 < \theta \leqslant \pi/2$, and by the factor $2/(1 + |\cos\theta|)$ when $\pi/2 \leqslant \theta \leqslant \pi$. This means, that when the temperatures of the beam source (T_{AB}) and of the gas cell (T_{PL}) are equal, the fraction of fast collisions in the cell is appreciably greater than in the atomic beams crossing at $\theta < \pi/2$. In endothermic reactions occurring in of fast collisions, $v_{col} \gg v_0$, the behavior of the distribution function $F_\theta(v_{col})$ is asymptotically exponential and the rate constant is characterized by the exponential factor

$$k = k'(v_0 \cos\theta)\exp\left(-\frac{bv_{th}^2}{v_0^2}\right), \quad v_{th} > v_0,$$

$$b = 1 \quad \text{for } 0 \leqslant \theta \leqslant \frac{\pi}{2}, \tag{3.10}$$

$$b = (1 + |\cos\theta|)^{-1} \quad \text{for } \frac{\pi}{2} \leqslant \theta \leqslant \pi,$$

where k' is a power function of v_0 and $\cos\theta$, and v_{th} is the threshold velocity.

It is clear from (3.3) that k depends significantly on the angle θ. For $\pi/2 < \theta < \pi$, a change in the argument of the exponential, e.g., at $v_{th} = 2v_0$, produces an increase in k by approximately an order of magnitude as θ increases from $\pi/2$ to π. For $0 \leqslant \theta \leqslant \pi/2$, the argument of the exponential in (3.10) is constant. We also note that the ratio of the arguments of the exponential $\exp(v_{col}^2/v_0^2)$ in the distribution functions corresponding to the effusive and gas-dynamic sources at the same temperature T is equal to 2. This can be interpreted as a reduction in the 'effective' temperature T of the beam of either kind as compared with the source temperature for threshold reactions. The efficacy of the threshold collision process as a whole increases monotonically as θ increases fro 0 to 180°. We note that the determination of the rate constant $k(\theta)$ as a function of θ in a beam experiment with a fixed temperature T of effusive sources is an analog of the determination of the rate constant as a function of temperature.

It is clear from Fig. 5 that, for a single beam ($\theta = 0$), the average value of v_{col} is reduced by a factor of 2 as compared with the case of the gas cell. In the figure, the range $\pi/2 < \theta < \pi$ corresponds to the case of plasma. Rigorous calculations show that the factor is 2.7. The mean collision rate in the atomic beam is thus lower by a factor of 2.7 than it is in the beam source, and this corresponds to a reduction in the mean collision energy by a factor of 7.3. For a source temperature of 400 K, which is typical of

alkali-metal atoms, the mean collision energy is found to be $\bar{E}_{col}=0.005$ eV. Such collisions are often referred to in the literature as subthermal and constitute an intermediate case between thermal collisions with $E_{col}=0.1-1$ eV and cold collisions with $E_{col}<0.001$ eV in experiments with laser cooling and confinement of particles.

4. CHEMI-IONIZATION IN COLLISIONS OF RESONANTLY EXCITED ATOMS AND THE SODIUM PARADOX

4.1. The type of studies of elementary processes

The type of studies of elementary processes undertaken in low-temperature plasma physics is largely dictated by the needs of applied physics. This in turn presupposes rapid theoretical interpretation and purposeful utilization of the experimental results. In low-temperature plasma physics, chemi-ionization reactions are traditionally regarded as providing an effective channel for the production of molecular ions. Applications of these reactions in optogalvanic spectroscopy, isotope separation, preionization in high-pressure discharges, and so on have all been proposed.

Chemi-ionization processes with appreciable rate constants k are being incorporated in an increasingly rigorous manner in transport equations for low-temperature plasmas. This refers in the first instance to studies involving inert-gas and alkali-metal atoms in the lowest of all the possible (resonance) excited states because of the extensive applications in science and technology. Two possibilities are then found to arise (see, for example, Ref. 46). They are:

(1) Total excitation energy greater than the ionization potential of an individual atom ($\Sigma U^* > U_i$).

(2) Total excitation energy smaller than the ionization potential ($\Sigma U^* < U_i$).

Case (1) includes the ionization of the atoms of hydrogen, inert gases, the halogens, nitrogen, and oxygen, whereas case (2) includes the ionization of alkali-metals, rare-earth elements, uranium, and most metals.

4.2. Experimental methods of studying chemi-ionization

Ionization during the excitation of cesium vapor in a space-charge limited cesium diode was reported[5] in 1930 and was interpreted as associative ionization. Although this method is difficult to modify for quantitative measurements, it has been used until quite recently whenever there was a need for recording elementary light absorption, followed by ionization, e.g., in the so-called heat pipe,[60] in estimates of the relative contribution of different excited states to ionization,[61] and in controlling laser-radiation parameters.[80] The first series of quantitative measurements of the rate constants for (2.2) was performed in the 1970s on group one elements. These publications proposed and implemented a method of optical excitation of a medium under the conditions of radiative transfer, in which volumes of the order of 100 cm^3 could be uniformly excited.[46] The advent of tuneable lasers provided a further stimulus to such atomic beam[54,62] and gas cell[49,63] experiments. However, such studies of resonantly excited alkali-metal atoms appear to have been confined to sodium atoms. The concentration of excited atoms was determined by fluorescence and photoionization methods, whereas the concentration of ground-state atoms was found from photoionization and the effective excited-state lifetime.[50,54,62] Ionization in an external electric field is widely used to determine N^{**} in studies of highly-excited atoms. In recent work, reaction (2.2) has been investigated for sodium, using Doppler velocity selection of excited atoms. In principle, this method enables us to investigate not only the rate constant and the cross section for the process as functions of particle energy,[65–67] but also the distribution of the resulting molecular ions over the vibrational states, using an additional ion photodissociation channel.[68] We can thus lower the energies down to $E\approx 0.005$ eV with an energy resolution of $\Delta E\leqslant 0.005$ eV, which corresponds to an effective temperature $T=20$ K (Ref. 67). In this method of velocity selection of excited atoms, the rate constant k is a function of the angle θ between the directions of laser and atomic beams, and is a minimum for $\theta=90°$. We note that, by using a monodirectional thermal beam to investigate chemi-ionization processes within the beam itself we at the same time significantly reduce the relative collision energy in comparison with the thermal energy of the beam source (Fig. 5). A record result was obtained in 1988: the AI rate constant of sodium was measured at $T=0.001$ K, using laser cooling and confinement in an atomic beam.[43] Moreover, polarized laser radiation has been used for the optical excitation atoms as a means of obtaining information on the individual magnetic sublevels of excited states and of determining the symmetry of the quasimolecular terms of X_2^* that are effective in chemi-ionization.

Mass selection of ions produced in these reactions can be carried out with quadrupole[64] and time-of-flight mass spectrometers.[62] Quadrupole mass spectrometers have high mass resolution, whereas time-of-flight measurements have higher threshold sensitivity and can be used to analyze reaction products with good time resolution. Electrons, which are also released during the chemi-ionization of excited particles, can be examined by electron spectroscopy (ES) with energy resolution $\Delta E=0.02$ eV, which means that it is possible to observe the vibrational-rotational structure of the resulting molecular ions.[69] ES methods are thus another way of selecting the states of molecular ions, in addition to the mass-spectrometric method. All these methods are used in studies of both quasimetastable (long-lived) and short-lived excited atoms.

The effect of the polarization of radiation on the AI exit channel was first investigated in Ref. 70 where the example of associative ionization of resonantly-excited sodium atoms was used to show that the yield of molecular ions was a maximum when the atomic beam was parallel to the polarization vector of the exciting radiation (these experiments employed linearly polarized light). The ion yield was found to fall to 60% of maximum for $\theta\approx 60°$, where θ is the angle between the radiation polarization vector and the direction of the atomic beam. Subsequent measurements[71,72] confirmed the results reported in Ref. 70.

Atomic spin alignment can also influence Penning ionization. A well-known example is that of ionization in asymmetric collisions between metastable helium atoms and ground-state rubidium atoms:

$$He(2^3S_1)+Rb(5^2S_{1/2})\rightarrow He(1^1S_0)+Rb^+(4^1S_0)+e. \quad (4.1)$$

The total electron spin in the initial states of the atoms is $S_1=1/2,1,3/2$ and the total spin in the final states is $S_2=1/2$. According to Wigner's rule, only 1/3 of all collisions can therefore result in ionization. The yield of charged reaction products should therefore rise appreciably when the spins of the colliding particles are antiparallel, and this has been confirmed experimentally.[73] It is important to remember that we can speak of the conservation of total spin only in the case of $L-S$ coupling between orbital and spin angular momenta for which the spin angular momentum is a 'good' quantum number.

According to Ref. 74, the cross section for Penning ionization at thermal velocities can be written in the form

$$\sigma_{PI}=f_{spin}P_{PI}\sigma_{cap}, \quad (4.2)$$

where f_{spin} is a statistical factor that represents the probability that the process is allowed by the total electron spin of the system of colliding particles, P_{PI} is the probability of ionization in an elementary collision event ($P_{PI}\approx 1$), and σ_{cap} is the cross section for the polarization capture of a particle in the attractive potential well for small nuclear separations. Like the statistical weight of the excited state, f_{spin} can be expressed in terms of the spin parameters of particles, so that the cross section σ_{PI} may be expected to depend on the statistical weight of the final excited state in the chemi-ionization reaction. This has been demonstrated experimentally,[75] for the reaction

$$He(2^1S_0)+Cs\rightarrow He(1^1S_0)+Cs^{+*}+e. \quad (4.3)$$

According to Ref. 75, the energy levels of the cesium ions with low statistical weights are less likely to be excited than levels with high statistical weights. This observation was also subsequently confirmed by the same research group for closely-spaced doublet states of excited ions in collisions of group two atoms with with metastable inert-gas atoms. Chemi-ionization has also been investigated in inert-gas plasmas by plasma electron spectroscopy[76] and, of course, mass spectrometry.[77] In the latter cases, a satisfactory result requires careful choice of experimental conditions, plasma geometry, pressure, degree of ionization of the medium, optimum design of the system used to select charged particles from plasma, and so on. Sufficiently reliable separation of chemi-ionization channels for different initial states of the excited atom can be achieved by selective laser excitation of after-glowin plasma. We conclude that the level of international standards in experimental studies of chemi-ionization is very high.

Analysis of existing experiments on collisional ionization of atoms and molecules at thermal energies enables us to formulate the basic conditions that must be satisfied by measurement procedures and technologies. Beam experiments are easier to interpret, and further processes in which charged particles are emitted are then easier to take into account. Mass-spectrometric and electron-energy analyses are simpler under these conditions, and ultrahigh vacuum allows the exclusion of readily ionized impurities with high reaction rates.[7,78] Cryogenic screens can be used in beam experiments to reduce, quite substantially, the effect of thermal radiation on excitation selectivity. Moreover, when the signal level is low, beam experiments require individual-particle counting with adequate time resolution and long-term storage if additional information on process kinetics is to be acquired.

Laser excitation with Doppler velocity selection of collision partners in beam experiments enables us to proceed from measurements of the effective reaction rate constants to determinations of cross sections. Unfortunately, continuously-operating tuneable lasers have not been widely used (with the exception of sodium) in selective excitation in experiments of this kind because of their limited tuning range and the energy parameters of radiation produced by them. Pulsed lasers are the most effective means of securing the necessary output power levels and tuning range between UV and IR. Moreover, when time resolution is high enough, excitation by laser pulses offers additional possibilities for studies of the kinetics of the processes under investigation. This requires automated systems for the control of laser radiation parameters and signal acquisition. The excitation system must have a wide power output range in order to ensure saturated transitions in studies of collisions between excited particles. An important problem in ionization experiments is the determination of the absolute concentration of initial reagents in excited and ground states, which are preferably measured by a number of independent methods. In the case of beam experiments, the concentration of Rydberg atoms is found from the measured fluorescence intensity or absorption coefficient for the analyzing radiation, which are are usefully complemented by field ionization whose efficiency approaches 100% for high excited states.

4.2.1. Inert gases. The theoretical paper by Garrison *et al.* that appeared in the 1970s and had a considerable influence on low-temperature plasma physics, reported calculations of the cross sections for reactions (2.2) and (2.3) with the participation of metastable helium atoms. The total cross section of $He(2^3S)$, evaluated over both channels for collision energies in the range 0.01–0.13 eV was found to agree to within experimental error ($\pm 30\%$) with beam[81,82] and plasma[83] experiments. However, the branching ratio $\sigma_{AI}/(\sigma_{AI}+\sigma_{PI})=0.46\pm 0.006$, obtained in beam experiments for (2.2) and (2.3), at collision energy $E=0.033$ eV, was very different from the calculated value.[80] The data obtained for γ in Ref. 80 were subsequently critically examined in Ref. 84. The result was a new value of γ that lay in the range 0.10–0.14, depending on the assumptions made about the transmission of the centrifugal barrier $\Delta U=0.7$ eV on the potential curve of X_2^*. Similar values were also obtained by plasma electron spectroscopy in experiments with decaying plasmas.[76,84] Experimental data reported in Refs. 81 and 82 for $E<0.1$ eV show that $\sigma_{AI+PI}\sim E^{-0.38}$, which is close to the func-

tion $\sigma = E^{-1/3}$ obtained in the polarization capture model for the attractive van der Waals type potential.

The polarization capture rates, calculated for the pairs He(2^3S),He(2^1S) and He(2^1S),He(2^1S) with allowance for Wigner's rule and the indistinguishability principle in collisions between identical particles, are found to be higher than for He(2^3S),He(2^3S), which is in agreement with the experiment reported in Ref. 76. Hence it follows in particular that the calculated or measured rate constants for reactions (2.2) and (2.3) must significantly depend on the relative populations of metastable states in the reaction entrance channel. For the decaying plasma, the main component of metastable states are the triplet states He(2^3S). This is so because the singlet atoms He(2^1S) are readily deactivated by electron impact in times of the order of 10^{-4} s. In the active phase of the discharge and early afterglow, the main contribution to chemi-ionization is provided by singlet metastable states. The He_2^+ ions produced in (2.2) occupy the upper vibrational states. In beam experiments, the ions take about 5×10^{-6} s to reach the collector, so that vibrationally excited molecular ions with lifetimes shorter 5×10^{-6} s are not recorded. In plasmas, the upper vibrationally-excited states of He_2^+ can be deactivated with the dissociation of the ion. This suggests lower values of γ in mass-spectrometer diagnostics of plasmas at higher pressures. This may be one of the reasons for the discrepancy with the values of γ obtained in plasma experiments. According to measurements on decaying plasmas performed by electron spectroscopy[76] and by mass spectroscopy,[85] the ionization rate constants for binary collisions of metastable atoms of helium, neon, argon, krypton, and xenon lie in the range 10^{-9}–1.5×10^{-9} cm^3 s^{-1} at $T=300$ K. It was only for (2.2) with the participation of two metastable atoms Ne($^3P_2$) that the measured rate constants were found to be smaller by a factor of 3. The same data indicated that γ lay in the range 0.05–0.10, i.e., close to the values for helium[81,82] and for the asymmetric process Ar*+Kr* (Ref. 81). In the latter case, the rate constant is $(3.1\pm0.6)\times10^{-9}$ cm^{-3} s (Ref. 81). The function $\gamma(E)$ is plotted in Fig. 6 for 2He*, He*Ne*, and Ar*Kr* collisions.

Currently available published data enable us to draw two important conclusions about low-temperature plasmas: (1) the ionization rate constants for binary collisions of metastable inert-gas atoms at room temperature are of the order of 10^{-9} cm^3 s^{-1}, and the main ionization channel is then the production of atomic ions and (2) at energies below 0.1 eV (see Fig. 6), the magnitude of γ increases with decreasing energy E. The relative yield of molecular ions is therefore greater in cryogenic plasmas. In view of this, it is interesting to consider recent experimental and theoretical studies[86] of binary collisions between metastable helium atoms at thermal and subthermal energies by high-resolution electron spectroscopy. These experiments employed a single beam of metastable atoms ($E=0.0016$ eV) and two crossed beams ($E=0.061$ eV; see Sec. 3). The effective reduction—by an order of magnitude—in collision energy was found to correspond to a substantial reduction (from 62 to 17) in the number of partial waves that had to be taken into account in the cross section, and

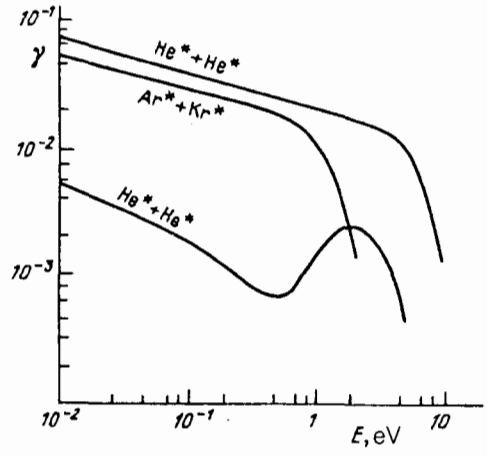

FIG. 6. Branching ratio γ for reactions (2.2) and (2.3) as a function of the particle energy according to beam measurements.[81]

allowed the observation of the structure of the electron spectrum due to interference between incident and scattered partial waves in the reaction entrance channel.

The total cross section for reactions (2.2) and (2.3) found in these experiments was $\sigma(0.033\text{ eV})=106\times10^{-16}$ cm^2 for the pair He(2^3S),He*(2^3S), which is in good agreement with published data. It was also found that $\sigma\sim E^{-\alpha}$ where $\alpha=0.33$ for $10^{-4}\leqslant E\leqslant5\times10^{-3}$ eV and $\alpha=0.27$ for $0.03\leqslant E\leqslant0.09$ eV. The measured relative cross sections for the He*(2^1S),He*(2^3S) and He*(2^3S),He*(2^3S) reactions in the case of single and crossed beams were found to vary between 2.7 and 2.1, which on the whole was in agreement with the ratio of the polarization capture cross sections.

4.2.2. Metal atoms. Between 1975 and 1985, many laboratories began studies of chemi-ionization of resonantly-excited alkali-metal atoms. It was found that the differences between beam and gas-cell (plasma) data were significantly greater than could be acsribed to experimental uncertainties alone. The validity of published values of the necessary constants ("sodium paradox"[55]) was therefore immediately questioned. The entire situation was analyzed in detail in Ref. 55 and it was shown that the spread in the published experimental results could be ascribed at least in part to the properties of the velocity distribution of the atomic excitation function $F(v)$ in different types of experiment. Below, we present new data, obtained mostly after 1986. Calculations of $F(v)$ (see Sec. 3) performed for the gas cell (plasma) have shown that this function was different from the distribution for the single beam, with the crossed beams occupying an intermediate position in this respect (see Fig. 5). For equal temperatures of the beam source and the gas cell, the distribution $F(v)$ contains more fast particles in the case of the gas cell. A model AI cross section was used in Ref. 55; according to Ref. 87 the AI cross section increases with energy near the threshold (a repulsive quasimolecular potential was considered). Recent work[65,66] has demonstrated a threshold-type behavior of the cross section for

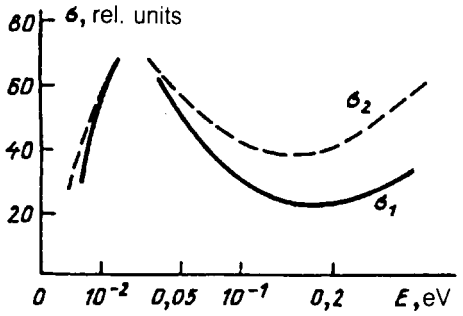

FIG. 7. The AI cross section for $Na(3^2P)+Na(3^2P)\rightarrow Na_2^+ + e$ in the energy range 0.3–0.003 eV: σ_1 and σ_2 refer to parallel and antiparallel atomic spin orientations. Mean: $\bar{\sigma}=\sigma_1+\sigma_2$.

$E\geqslant 0.1$ eV, which agrees with Ref. 87, and also the presence of a cross section peak in the energy range $0.005\leqslant E\leqslant 0.1$ eV whose size is comparable with $\sigma(0.3\text{ eV})$ (Fig. 7). Hence it follows that, for sodium, existing evidence confirms multichannel AI in (2.2). This had been proposed for helium in Ref. 88.

Recent high-resolution electron spectroscopy[89] shows that the distribution of molecular ions produced in (2.2) over the vibrational states is independent of the polarization of the colliding particles, and that a population peak is observed for $v=2$ and $v=3$. These data also indicate that, in a monodirectional atomic beam with a reduced number of 'fast' atoms, there is only one ionization channel that is due to the crossing of the ionic molecular continuum by the initial quasimolecular term for vibrational quantum numbers $v<6$.

The good agreement between the experimental data in Ref. 89 and the theory in Refs. 90 and 91 enables us to identify the intial quasimolecular term as $^3\Sigma_u^+$, i.e., an attractive term with $R_c\approx 5$ a.u..

New AI channels become available in the plasma (gas cell) of crossing or counter propagating beams.[92] They are due to the crossing of the ionic and covalent molecular terms in the region of the 10th vibrational state of Na_2^+ (the $^1\Sigma_g^+$ term[90] or the $^1\Sigma_u^-$ term[55]). This may also be responsible for the complex character of the function $\sigma(E)$ obtained in Ref. 66 by polarization spectroscopy used in conjunction with laser velocity selection of excited atoms. The alternative approach is to use the model of Ref. 21, which suggests that $\sigma(E)$ may acquire a set of ionization resonances when the condensation of vibrationally excited terms of the quasimolecule Na_2^* interacts with the low-lying vibrational state of the ion Na_2^+. The peak observed on $\sigma(E)$ in Ref. 66 may actually be the envelope of a large number of unresolved narrow resonances. We note that, to explain the measured peak width, an additional assumption had to be introduced in the model of Ref. 21: it was assumed that the autoionization AI width decreased with decreasing R_c. The authors of Ref. 67 used their own complicated procedure to reconstruct $\sigma(E)$ from the polarization dependence of the AI signal, and obtained a set of cross sections for intermediate quasimolecular states with different values of the projection of the total electron angular momentum of the system. However, the conclusion[67] that the total AI cross section was independent of the particle energy in a wide range of energy values does not agree with the data in Ref. 66 or the conclusions of Ref. 55. The theory developed in Ref. 67 also did not take into account depolarizing collisions or possible inelastic transfers of excitation from the initial $2Na(3^2P)$ term to the $Na(3^2S,4^2D)$ term with characteristic cross sections $\sigma=10^{-15}$ cm^2. The AI cross section σ_{AI} was calculated in Ref. 44 by semiclassical methods for collision energies in the range 10^3 K$\geqslant T\geqslant 10^{-4}$ K, and it was concluded that σ increased monotonically with decreasing energy. It is known, however, that nuclear motion remains classical on the approach stage, but only down to $T\geqslant 1$ K. Hence it is a relatively unexpected result that the data obtained in Ref. 44 agree with the measurements reported in Ref. 43 for $T=10^{-3}$–10^{-4} K. The order-of-magnitude result $\sigma\approx 10^{-13}$ cm^2 suggests that, in addition to the resonance noted in Ref. 66, there is a narrow giant resonance on the function σ for $E\rightarrow 0$. On the other hand, the properties of collisional ionization at subcryogenic temperatures remain practically unknown.

A new aspect of 'very cold' collisions between two resonantly-excited sodium atoms held in a light trap is discussed in a recent paper.[93] It is suggested in that paper that the production of Na_2^+ ions in low laser intensities ($N^*/N_0\sim 10^{-3}$) can be considered as the following four-stage process: (1) $Na+Na+h\nu_1\rightarrow Na^*+Na^*$, (2,3) the particle pair moves in the attractive potential of the quasimolecule with the simultaneous absorption of the laser photon $h\nu_2$ and the associated production of a pair of resonantly excited atoms ($Na+Na^*+h\nu\rightarrow Na^*+Na^*$), and (4) the two excited atoms interact and produce the molecular ion. The proposed aproach opens up a way of controlling the AI process between wide limits by varying the incident intensity and the photon energies $h\nu_1, h\nu_2$. For effective collision temperatures of 10^{-6} K, the rate constant for this type of multistage process can range[93] between 10^{-8} and 10^{-9} cm^3 s^{-1} which is greater than the value measured at $T=10^{-3}$ K by two or three orders of magnitude.

Thus, on the one hand, sodium is the most extensively investigated example of (2.2) for metal atoms, whilst, on the other hand, newly published data are not entirely free from internal contradiction. Table I lists the AI rate constants of reaction (2.2) for sodium.[55] The corresponding values for other alkali metals can be found in the review literature.[3,4] These data can be used directly for low-temperature plasmas because they are the result of measurements on gas cells in which the atoms are excited under the conditions of resonant radiation transfer. The detailed examination given in Ref. 46 of radiation transfer under isotropic broad-spectrum primary illumination reveals that this type of excitation is valid in quantitative studies of endothermic AI processes. A further significant point here is the Maxwellian velocity distribution of the excited atoms, which means that optical diagnostics can be used for excited atoms. Such studies have much in com-

TABLE I. Corrected[55,92] AI rate constants for the process $Na(3^2P)+Na(3^2P)\rightarrow Na_2^+ + e$.

Experimental conditions	Beam source temperature, temperature of saturated vapor, K	k, 10^{-11} cm^3 s^{-1}
Gas cell (plasma)	550	3,8 [1]
Beams crossing at 90°	570	3,4 [54]
Single beam	580	0,03 [62]

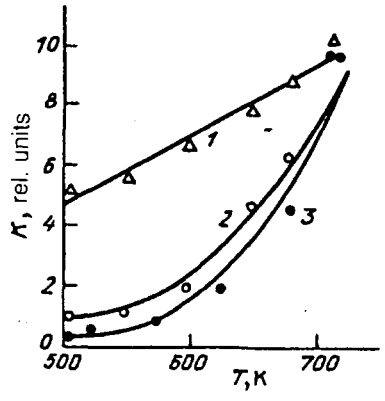

FIG. 8. Temperature dependence of the AI rate constant of cesium at $T=713$ K according to Refs. 46 and 61: *1*—$Cs(6^2S)+Cs(8^2P)\rightarrow Cs_2^+ + e$, *2*—$Cs(6^2S)+Cs(7^2P)\rightarrow Cs_2^+ + e$, *3*—$2Cs(6^2P)\rightarrow Cs_2^+ + e$. Solid curves—calculated from the formula $k\approx(1+\Delta U/kT)e^{-\Delta U/kT}$; $\Delta U=U_i-D_c^+-\Sigma U^*$, D_c^+—dissociation energy of the molecular ion Cs_2^+.

mon methodologically with early measurements of the photoionization cross sections of resonantly-excited atoms, and have been carried out with the same apparatus.

The analysis of experimental data given in Ref. 46 (Table II) does not take into account fine level splitting, i.e., it assumes that $k_{1/2,1/2}=k_{3/2,3/2}=k_{1/2,3/2}$, where the subscripts are the values of the quantum number j of the colliding excited atoms. It is important to note, however, that for the resonant 3^2P states of sodium, the ratio $k_{3/2,3/2}/k_{1/2,1/2}$ varied between 10 and 4 in the resonant flux-density range 10^4–10^6 W·cm^{-2} (see also the beam measurements reported in Ref. 95).

We know of no measurements of the reaction rate of (2.2) in the case of lithium. Since the reaction energy defect estimated from tabulated data is about 0.5 eV, it may be expected that the corresponding reaction rate constant should be 10^{-15}–10^{-16} cm^3 s^{-1}. The activation energies listed in the Table II were obtained from the measured values of the temperature function $k(T)$. When $\Delta U\neq 0$, the expression for the reaction rate contains the factor $\exp(-\Delta U/T)$ which largely determines the temperature function $k(T)$. Strictly speaking, this is valid only for cross sections the are slowly-varying functions of the energy of relative motion of the colliding particles. However, the exponetial factor appears in more realistic cases of cross sections as well. The strong (exponential) dependence of the reaction rate for AI from resonant levels of alkali-metal atoms must be taken into account in any real plasma experiment. The temperature can thus reach $\sim 10^3$ K in the plasma of the low-voltage arc discharge in cesium. The AI rate constant of resonantly excited cesium atoms, for example, is greater by two orders of magnitude as compared with the data in Table II, reaching 10–11 cm^3 s^{-1}.

TABLE II. Rate constants and activation energies ΔU for binary collisions of resonantly-excited alkali-metal ions.[3]

Collision partners	ΔU, eV	k, cm^3 s^{-1}	k/v_{col} *), cm^2
$2Cs(6^2P)$	0,33 ± 0,04	$(2\pm 0{,}2)\cdot 10^{-13}$, $T=425$ K	$3{,}4\cdot 10^{-18}$
$2Rb(5^2P)$	0,20 ± 0,03	$(3{,}2\pm 0{,}4)\cdot 10^{-13}$, $T=470$ K	$0{,}64\cdot 10^{-17}$
$2K(4^2P)$	$\lesssim 0{,}1$	$(9\pm 2)\cdot 10^{-13}$, $T=500$ K	$1{,}3\cdot 10^{-17}$
$2Na(3^2P)$	—	$(3{,}8\pm 0{,}4)\cdot 10^{-11}$, $T=580$ K	$3{,}8\cdot 10^{-16}$
$2Li(2^2P)$	$\gtrsim 0{,}5$	10^{-15}—10^{-16}	—

*) v_{col} is the mean relative velocity for collisions at temperature T.

Ionization in binary collisions between atoms in low-lying excited states other than resonant states was first investigated in Ref. 61 in the special case

$$Cs(6^2P)+Cs(5^2D)\rightarrow Cs_2^+ + e. \qquad (4.4)$$

When $T=500$ K, the reaction rate is 1.5×10^{-10} cm^3 s^{-1}. This high rate constant is due in the first instance to the much lower activation energy (energy threshold) of the reaction. Figure 8 shows the temperature dependence of the rate constant for AI with the participation of atoms in low-lying excited states (experimental data from Ref. 61, analyzed in Ref. 46). It is clear that AI with the participation of atoms in low-lying excited states of alkali-metal atoms must be treated above all as a process with a threshold. Hence it follows, in particular, that the cross sections obtained simply by dividing the measured rate constant by the mean relative velocity of the particles (last column in Table II) are not acceptable. The efficacy of threshold AI processes depends significantly on the shape of the particle velocity distribution, so that published data on such processes are, strictly speaking, admissible only of the corresponding conditions are the same. When the conditions are different, the data must be re-examined, and this can only be done if we know the corresponding terms of the quasimolecules and the molecular ion. The yield of AI reactions with an energy threshold is largely governed by the quantity $\Delta U/T$ where T is the temperature of the neutral component of the plasma, gas cell, or beam source. When this parameter is large, the reaction rate in plasma is much greater than the rate of the same reaction in the thermal beam. Hence AI reactions with large ΔU are probably best investigated for the gas cell or the gas-dynamic

beam. The reaction yield in a single effusive atomic beam is the lowest of all the special cases considered above. It is also possible to give an opposite example in which the yield increases as we pass to the beam experiment. For this to happen, the characteristic thermal energy must exceed the threshold value, and the cross section must fall more rapidly than v_{col}^{-1}.

Since the AI reaction rate constant is difficult to calculate theoretically, measurements of k and the consequent improvements in the model parameters will be of immediate interest, at least for the next few years. Until recently, quantitative data on AI in binary collisions between metal atoms in low-lying excited states (other than the alkali metals) were available for mercury and cadmium. The lower triplet states of these atoms can be populated by a combined optical and collision method[96] in which collisions of the second kind between optically excited atoms $X(n^3P_1)$ and molecules produce the effective population of $X(n^3P_0)$ states. The rate constant for the process $Hg^*(6^3P_0) + Hg^*(6^3P_0) \rightarrow Hg_2^+ + e$ $k_{AI} = (4.0 \pm 0.8) \times 10^{-10}$ cm^3 s^{-1}, $T = 295$ K, which is in good agreement with calculations based on polarization capture theory and enables us to treat this process as having no threshold. The rate constant obtained earlier for the process $Hg^*(6^3P_0) + Hg^*(6^3P_1) \rightarrow Hg_2^+ + e$ was found to be[97] $k_{AI} = 1.2 \times 10^{-9}$ cm^{3}s^{-1} at $T = 400$ K, which is greater by a factor of about three than the result of the polarization capture calculations. For the cadium atom, the effective value of k_{AI} for the set of $5^3P_{0,1,2}$ states was 4×10^{-12} cm^3 s^{-1} at $T = 575$ K. This is significantly lower than the result of polarization capture calculations, showing that in this case the process has a threshold. For binary collisions between metal atoms in excited or resonant states, the main ionization channel is AI ($\gamma = 1$), i.e., we have a situation that is the inverse of that in inert gases.

Ionization has also been recorded for the mixtures Cs–Hg, Cs–Cd, and Rb–Cd excited optically to the n^3P_1 resonant states of the second component (see Ref. 46). Such systems are interesting because they offer the prospect of UV detection in which these mixtures are used in low-voltage selective receivers of UV radiation from resonant transitions in group two elements. Quantitative data on reaction rates for these processes are available only for

$$Cs(6^2S_{1/2}) + Hg(6^3P_1) \rightarrow Cs^+(5^1S_0) + Hg(6^1S_0) + e, \quad (4.5)$$

for which $\sigma = (6 \pm 2) \times 10^{-14}$ cm^2 which is greater by more than an order of magnitude than expected from the Katsuura–Smirnov model. One of the reasons why the experimental result is too high (by a factor of 3.3) is that, according to Ref. 46, the ion current was not normalized correctly. Moreover, the experimental results may have been affected by secondary processes that produced additional ionization of the medium.

Table III lists experimental data on Penning ionization with the participation of metastable inert-gas and alkali-metal atoms [reactions (4.1)], obtained for pulsed-discharge afterglow from measured values of the total quenching rates of metastable states. It is clear from the table, and was noted above, that, since total spin angular momentum must be conserved, the magnitude of k_{AI} is greater for $He(2^3S_1) + Cs(6^2S_{1/2})$ than for $He(2^1S_0) + Cs(6^2S_{1/2})$. Such reactions attracted the attention of researchers in 1973 since it had been suggested that they had a decisive role in producing population inversion in lasers employing ionized cadium and zinc vapor.[102] However, such lasers have not joined the range of gas lasers available so far. Moreover, there is published evidence that electron-atom collisions play an important role in the population of the upper laser level under these conditions.[103]

TABLE III. Total rate constants for the quenching of rare-gas metastable atoms by ground-state alkali-metal atoms.

Collision partners		k, 10^{-10} cm^3 s^{-1}		
		Theory, $T = 300$ K	Experiment	
$He(2^3S)$	Zn	9,2 [98]	5,1 ± 1,5	[99]
	Na	8,1 [98]	7,7 ± 1,5	[99]
	K	9,0 [98]	12,0 ± 2,4, $T = 350$ K	[99]
	Rb	9,1 [98]	4,5 ± 0,9	[99]
	Cs	9,7 [98]	4,4 ± 1,6, $T = 450$ K	[100]
$He(2^1S)$		—	15 ± 6	[100]
$Ne(^3P_0)$	Cs	—	31 ± 9, $T = 450$ K	[101]
$Ne(^3P_2)$		—	30 ± 9	[101]

Heavier cluster ions are produced in plasmas at pressures greater than 0.01 mm Hg because of three-particle conversion of atomic ions, the nonresonant charge transfer between the atomic ion and the molecules, and ion-molecule transfer processes. The rates in the first two channels are comparable for $p > 10$ mm Hg (pairs of alkali-metal ions). For $p > 1$ mm Hg, the cluster ions $X_2^+, X_3^+, \ldots X_n^+$ may become the principal ionic component of the alkali-metal plasma with normal-component temperature $T < 1000$ K. In this connection, we note that chemi-ionization in collisions between excited molecules and resonantly-excited atoms of the same species, i.e.,

$$X_2^* + X^* \rightarrow X_3^+ + e \quad (4.6)$$

can also have appreciable effective rate constants.[104] Process (4.6) is interesting because it allows us, at least in principle, to produce cluster ions X_n^+ with predetermined composition by choosing the corresponding excited collision partners.

4.2.3. Molecular gases. Chemi-ionization processes involving excited molecules are of practical interest above all for the description of ionization kinetics in glow-discharge plasmas, afterglow plasmas, plasmochemical devices, and active laser media. Publications on these processes issued up to the beginning of the 80s are reviewed in Ref. 105 in which processes such as

$$N_2(X^1\Sigma_g^+, v_1) + N_2(Z, v_2) \rightarrow N_4^+ + e(v_1 \geqslant 13), \quad (4.7)$$

$$N_2(X^1\Sigma_g^+, v_1) + N_2(X^1\Sigma_g^+, v_2) \rightarrow N_4^+ + e(v_1 \approx v_2 \geqslant 32) \quad (4.8)$$

are looked upon as probable ionization mechanisms for the glow discharge[105–107] in molecular nitrogen, its afterglow, and the N_2+He mixture. In the above expressions, $N_2(Z,v_2)$ are highly-excited metastable states ($E_{exc} \approx 12.2$ eV). The influence of vibrational excitation of nitrogen molecules on ionization in a glow discharge was also examined in recent papers.[108–109] According to these data, the main ionization channel in the low-pressure nitrogen glow discharge is the AI process with the participation of nitrogen in $a'^1\Sigma_u^-$ and $A^3\Sigma_u^+$ states:

$$N_2(a'^1\Sigma_u^-)+N_2(A^3\Sigma_u^+)\rightarrow N_4^++e, \tag{4.9}$$

$$N_2(a'^1\Sigma_u^-)+N_2(a'^1\Sigma_u^-)\rightarrow N_4^++e. \tag{4.10}$$

The published rate constants for these processes were mostly obtained by fitting the data to the kinetic model of the positive column (afterglow plasma) so as to ensure the best agreement between calculated and measured plasma parameters. According to Refs. 108 and 109, the rate constants estimated in this way for (4.9) and (4.10) lie in the range $5\times10^{-11}-6\times10^{-12}$ cm^3 s^{-1} for (4.9) and $2\times10^{-11}-5\times10^{-12}$ cm^3 s^{-1} for (4.10) at gas temperatures of the order of 10^3 K. However the lower ionization constants reported in the more recent paper[109] is probably more reliable. The following upper limit for the degree of vibrational excitation of the $X^1\Sigma_g^+$ state of molecular nitrogen in reaction (4.7) is also proposed in Ref. 109: $v_1 \leqslant 20$. Similar estimates of the chemi-ionization rate constant of molecular gases are also available for CO-containing discharges.[110] The ionization balance in mixtures such as He–Co and He–CO–O_2 that are typical for the working media of powerful CO lasers was also discussed in Ref. 110. The best agreement between model calculations and measurements is achieved by assuming that the principal ionization mechanism in He–CO–O_2 mixtures is the following AI process:

$$CO(v>14)+CO^*(I^1\Sigma)\rightarrow C_2O_2^++e. \tag{4.11}$$

The authors of Ref. 110 were able to estimate the ratio of rate constants for (4.11) and for the transfer of excitation without ionization in collisions between $CO^*(I^1\Sigma)$ and the ground-state CO molecule. This ratio was found to be equal to 2 for liquid-nitrogen cooled discharges.

There is a vastly greater volume of quantitative data on the rate constants (and cross sections) of the Penning process in thermal collisions between metastable inert-gas atoms and CO, CO_2, H_2, O_2, M_2, and nitrogen-containing molecules. For all these pairs, the ionization rate constant decreases with decreasing energy in the range 0.03–0.1 eV. The order of magnitude of these constants is in the range 10^{-9}–10^{-10} cm^3 s^{-1} ($E \approx 0.03$ eV). These observations show that the above interactions result in the formation of intermediate states of the weakly-bound quasi molecule with a potential-well depth of 0.03 eV and that ionization occurs on the repulsive part of the interaction potential.

It was suggested in Ref. 111 that optical alignment of metastable helium atoms could be used to investigate reactions such as

$$He(2^3S_1)+M_2\rightarrow He(1^1S_0)+M_2^++e \tag{4.12}$$

with the participation of molecules. Actually, experiments on the ionization of CO, CO_2, and N_2O by optically oriented helium atoms were found to produce electrons with polarization close to the initial polarization of the metastable atoms.[112] The polarization transfer effect (conservation of total electron spin) was also noted in collisions between metastable helium atoms and nitrogen molecules.[113]

We note that, as in the case of reactions (2.2) and (2.3), which involve metastable inert-gas atoms, the efficacy of atom-molecule processes is different for single and triplet states and the ratio of the two tends asymptotically to unity for collision rates $v \gg 10^5$ cm $\cdot$ s^{-1}. It is then found that the exit channel of the reaction

$$A^*+M_2\rightarrow A+M_2^++e, \rightarrow AM_2^++e, \tag{4.13}$$

where A^* is a metastable atom and M_2 is a molecule, contains more than 90% of M_2^+:Ne ($^3P_{0,2}$)+N_2, CO, CO_2, and the isotope effect provides a substantial contribution. Finally the most commonly encountered practical case is that of the flame of hydrocarbon fuels in which the principal source of charged particles is the AI process

$$CH+O\rightarrow CHO^++e. \tag{4.14}$$

We note in conclusion that, in addition to Ref. 2 which was cited above, information on Penning ionization of molecules can be found in the review in Ref. 114.

5. CHEMI-IONIZATION PROCESSES INVOLVING RYDBERG ATOMS

5.1. Collisions between excited and ground-states atoms

Let us now consider the main properties of (2.4) and (2.5) within the framework of the DShMYa model[14,15] developed for the evaluation of the chemi-ionization constants and the electron energy spectrum produced in chemi-ionization. So long as the kinetic energy E of the colliding atoms remains smaller than the sum of the binding energy $E_i^*(n)$ of the excited electron and the energy ε of the emitted electron, only the channel (2.4) is energetically allowed. For higher values of E and nuclear separations $R_x \ll R \ll R_x^{**}$, the direct ionization channel opens up (R_x^{**} and R_x are the classical radii of the excited and ground-state atoms). For small nuclear separations, the system is described by a repulsive quasimolecular potenial $U_1(R)$ which is analogous to the $^2\Sigma_u^+$ potential curve of the molecular ion H_2^+ and the attractive potential $U_2(R)$ that corresponds to the $^2\Sigma_g^+$ state of H_2^+.

Ionization occurs as the system X_2^* passes from the repulsive term to the attractive term with simultaneous autoionization. One of the consequences of the DShMYa model for the relatively low values of the quantum number $n_{eff} \leqslant 10$ is that k increases with increasing n_{eff}, which corresponds to AI with energy threshold. This theory was developed after the publication of the first systematic experimental studies of the AI of Rydberg atoms, and has played a significant part in establishing this topic in atomic physics. Calculations based on the DShMYa model rely on the perturbation theory formalism. However, for $n_{eff} \geqslant 10$,

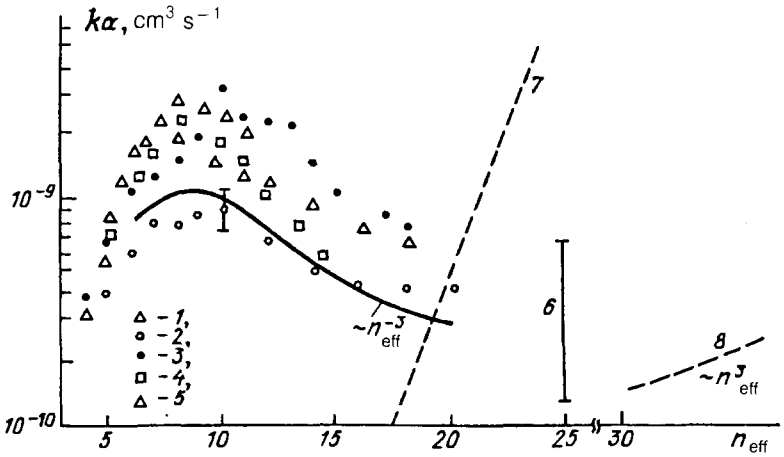

FIG. 9. Chemi-ionization rate constants for (2.4) and (2.5) as functions of the effective quantum number of excited states:[4] *1*—Li ($T=1100$ K), *2*—Na ($T=720$ K), *3*—Na ($T=600$ K), *4*—K ($T=660$ K), *5*—Cs (see text for details), *6*—range of values of k (Na(n^2l)+Na(3^2S), $l=0$, 1 and 2, $T=1000$ K; single effusive beam),[107] *7*—calculated using the model relying on electron capture to an autoionizing state of a negative ion (Na, $T=500$ K), *8*—qualitative form of $k(n_{\rm eff})$ according to the model relying on the scattering of a quasi-free weakly-bound electron in the sodium atom; solid curve—DShMYa model (sodium, effusive beam, $T=700$ K).[59]

the autoionization probability is close to unity, which means that it is doubtful whether k can be calculated by perturbation theory. A more rigorous model-based approach gives $k_{\rm eff}\approx\pi R_c^2 v_{\rm coll}$ for $n_{\rm eff}\geqslant 10$, where R_c is the nuclear separation for which the initial and final terms cross diabatically.

Figure 9 shows the chemi-ionization rates of highly-excited atoms, taken from the review literature.[4] In the case of lithium, sodium, pottasium and cessium, obtained with effusive atomic beams (Li, 1100 K; Na, 720 K), crossed beams (Na, 600 K), a single atomic beam (K, 660 K), and a gas cell (CS, 500 K). The rate constants are given in units of $k\alpha$, where

$$\alpha^{-1}\left(\frac{T_{\rm Na}M_{\rm A}}{T_{\rm A}M_{\rm Na}}\right)^{1/2},$$

where $T_{\rm A}$ is the temperature of the source (cell), $T_{\rm Na}$ is the temperature of the source of the effusive beam of sodium (720 K), and $M_{\rm A,Na}$ is the mass of the atoms of the element under investigation and of sodium, respectively. For processes with low values of $\Delta U/T$, this procedure means that we are dealing with results corresponding to the mean relative particle velocity $v_{\rm col}=1.1\times10^{-5}$ cm·s^{-1}. Within the framework of the DShMYa model, and typical experimental conditions, this is satisfied, strictly speaking, for $n_{\rm eff}\geqslant 15$. The dashed line shows the relative behavior of the function $\varkappa\sim n^{-3}$, which follows from the Fermi model for highly-excited states. For $n>10$ the measured ion current contains a contribution due to AI from low-lying levels of the excited atom, populated by a radiative cascade. Estimates show that this effect can be neglected for $n_{\rm eff}\leqslant 8$.

Figure 10 shows the function $\varkappa(n_{\rm eff})$ for the rubidum atom.[4] The effective quantum number was the determined for the system X*Y(Y*) from the relation

$$n_{\rm eff}=\left[2\left(U_{\rm i}-\sum U^*\right)\right]^{-1/2}, \qquad (5.1)$$

where $U_{\rm i}$ is the ionization energy of the primary excited atom and ΣU^* is the total excitation energy of the system X*Y(Y*) in atomic units. In other words, $n_{\rm eff}=1/2E_i^*$ where E_i^* is the binding energy in the intial state, measured from the energy of the ionic term ($R\to\infty$) of the the system XY^+. It is clear that, within the range of experimental error (at least for $n_{\rm eff}=4$–8), the measured chemi-ionization rates are not very dependent on quantum numbers l, j or the species of the colliding atoms. Recent calculations based on the DShMYa model that take into account the true velocity distribution of the atoms (Na, K) are in reasonable agreement with the "traditional" DShMYa model up to $n_{\rm eff}\leqslant 25$. On the other hand, there are some experimental facts that have not found an explanation within the framework of the model.

DShMYa model calculations of the rate constant for

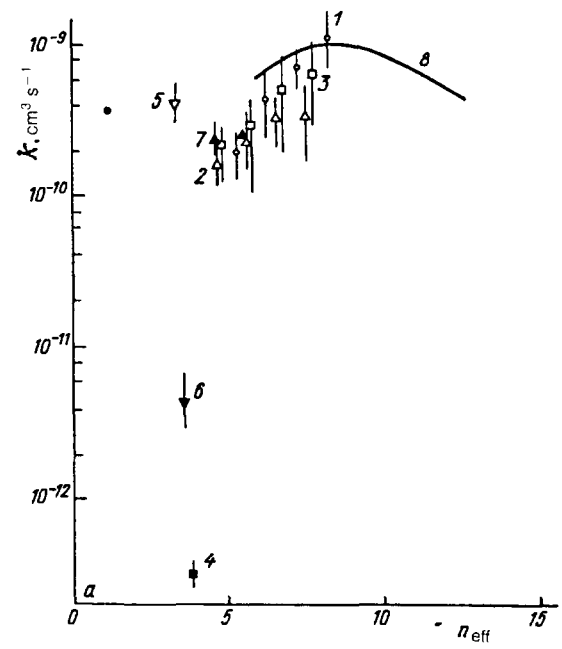

FIG. 10. Total chemi-ionization rate constant for (2.4) and (2.5) as a function of the effective quantum number for Rb, Hg, and Cd. *1*—Rb(n^2P)+Rb(5^2S) ($T=520$ K), *2*—Rb(n^2D)+Rb(5^2S) ($T=470$ K), *3*—Rb(n^2S)+Rb(5^2S) ($T=470$ K), *4*—Rb(5^2P)+Rb(5^2P) ($T=470$ K), *5*—Hg(6^3P_0)+Hg(6^3P_0) ($T=300$ K), *6*—Cd($5^2P_{0,1}$)+Cd($5^2P_{0,1}$) ($T=575$ K), *7*—Rb(n^2D)+K(4^2S) ($T=440$ K), *8*—DShMYa model calculations for Rb ($T=520$ K) (Ref. 15).

TABLE IV. Direct ionization cross sections for binary collisions of highly-excited and resonantly-excited atoms of rubidium, 10^{-13} cm^2 (T =450 K) (Ref. 64 and 100).

Collision partners	Experiment	Theory
Rb(6 ^{2}D) + Rb(5 ^{2}P)	8,4 ± 1,8	5
Rb(8 ^{2}S) + Rb(5 ^{2}P)	4,4 ± 1,4	5,12
Rb(7 ^{2}D) + Rb(5 ^{2}P)	4,4 ± 1,8	5,01

asymmetric AI with the creation of a heteronuclear molecular ion show that this constant may be higher than the corresponding result for the symmetric process if the ionization-energy difference between the colliding atoms is greater than the kinetic energy of the colliding particles. Hence it follows in particular that the results calculated in this way should be essentially different for the single beam and the crossed-beam system (gas cell). This conclusion, and also the fact that the potential $U^*(R)$ is different for homonuclear and heteronuclear quasimolecules, may offer an explanation for the ambiguity[115] in the measured rate constants for the asymmetric production of the $NaLi^+$ ion and the symmetric production of the Na_2^+ and Li_2^+ ions in crossed lithium and sodium beams.

The direct and associative ionization of the Rydberg hydrogen atoms colliding with ground-sate helium atoms was examined in Ref. 32 with allowance for energy transfer between an outer electron and the relative motion of the heavy particles:

$$X^*(n)+Y\rightarrow X^++Y+e,\rightarrow YX^++e. \qquad (5.2)$$

In contrast to Penning ionization, (5.2) produces the ion X^+ and not Y^+; for $n>20$ and $0.03\leqslant T\leqslant 0.3$ eV, direct ionization is the dominant process that also dominates collisions between highly excited atoms and atoms in low-lying states. Table IV shows measured and calculated cross sections for such reactions in the case of the rubidium atom ($\gamma\leqslant 0.1$).

We note that experiment does not confirm the relation $\sigma \sim E_i^*$ that follows from Ref. 2. The first absolute measurements of k_{AI} for (2.4) in the case of inert gases were reported in Ref. 117:

$$He(3^{1,3}P),\quad He(3^{1,3}D)+He\rightarrow He_2^++e. \qquad (5.3)$$

The cross section $\sigma=kv_{col}^{-1}$ for these reactions lies in the range 1.6×10^{-16}–20×10^{-16} cm^2. For states with $n_{eff}<3$, the AI cross section should depend on the individual characteristics of the original quasimolecular terms. For such levels, the effect of the "crossings grid" on the AI probability can be taken into account relatively simply: Fig. 11 shows the diabatic potential curves for the excited states of helium with $n\leqslant 7$. Figure 12 shows the energy dependence of the cross section for the 5^3P states of helium,[118] obtained in crossed-beam experiments. The He_2^* term crossings that contribute to the cross section are indicated in Fig. 12. A mark with the notation $5P\rightarrow X^2\Sigma_u^+$ indicates a diabatic reaction threshold and the solid curve was obtained by calculation.[119] Thus, we have to know the potential curves

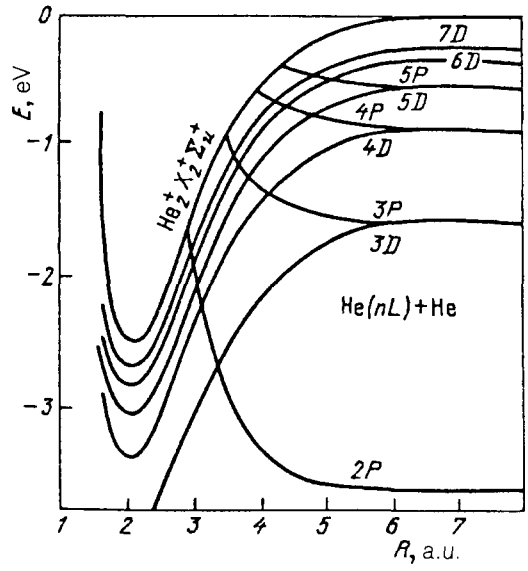

FIG. 11. Diabatic potential curves of the molecule He_2^* produced in He (n^3P,^{3}D), He collisions.[118] The states shown in the figure provide the maximum contribution to AI in primary excitation of the He(5^3P) state.

for the quasimolecule corresponding to a pair of excited and ground-state atoms for $R\rightarrow\infty$ before we can undertake a theoretical analysis of chemi-ionization. At this point we recall Ref. 120 in which experience with calculations of adiabatic potential curves for low-lying (resonantly excited) states was used to calculate intermediate (higher-lying) states of Na*Na.

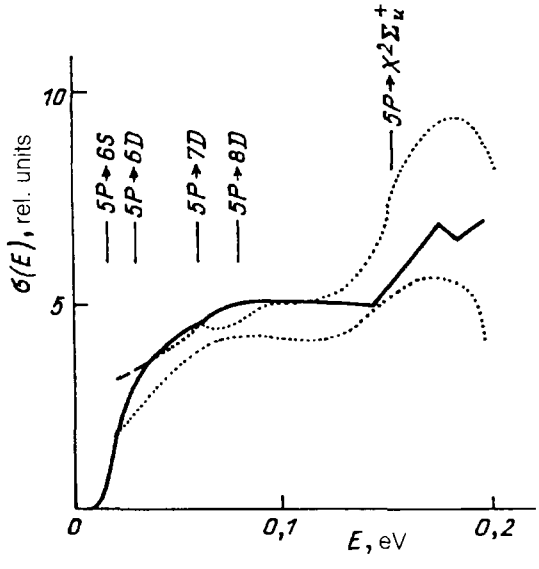

FIG. 12. AI cross section for the process He(5^3P) + He as a function of collision energy. Solid curve—calculated; arrow near the threshold corresponds to the 5P–6S quasicrossing of terms not shown in Fig 11 (Ref. 118).

TABLE V. Rate constants for the process (2.6) in the case of the rubidium atom.[111]

Initial excited state	k, $cm^3\ s^{-1}$	
	Calculation based on the Landau–Zener model	Experiment
$5\,^2D$	$0{,}75\cdot10^{-14}$	$(1{,}1\pm0{,}5)\cdot10^{-14}$
$7\,^2S$	$0{,}78\cdot10^{-13}$	$(1{,}0\pm0{,}5)\cdot10^{-13}$
$7\,^2P$	$0{,}002\cdot10^{-13}$	$3\cdot10^{-13}$
$6\,^2D$	0	$(1{,}1\pm0{,}3)\cdot10^{-12}$
$8\,^2S$	0	$3{,}9\cdot10^{-13}$

5.2. Binary collisions between highly-excited atoms

The calculated cross sections of hydrogen for (2.7)–(2.9) lie in the range 10^{-12}–10^{-11} cm^2 for $n_{eff}=10$–20 (Refs. 34–121) and their maximum values correspond to n_{eff} for which the mean kinetic energy of a highly-excited electron is comparable with the relative kinetic energy in atom-atom collisions. The total energy of the two HEAs is significantly greater than the ionization energy of an individual atom, which is similar to the collison of two metastable inert-gas atoms, considered above. The difference between these two situations is that in the latter case the gap between the original term of the quasimolecule and the first ionization potential contains a series of autoionizing states that can manifest themselves directly in the exit channel. The relatively few publications devoted to these processes usually report quantitative conclusions only for a particular ionization channel: associative ionization[35] or a pair of positive and negative ions.[124] According to Ref. 35, the calculated rate constant for the production of atomic ions in (2.8) is greater by an order of magnitude than the corresponding cross section for (2.7). This conclusion does not, however, agree with the measuements reported in Ref. 125 for $T\leqslant60$ K. Hence it follows in particular that the production of ionic molecular clusters proceeds with sufficient probability in collisions at subthermal energies. Figure 5 compares measurements made at $T=85$ K with calculated[34] probabilites of different ionization channels (2.7) and (2.8). We note the different temperature dependence of the two rate constants: in the former case, the rate constant increases with decreasing temperature whereas in the latter case it decreases. The increase in the total ionization rate constant with increasing n shown in the figure (for $v_{col}\ll1$) follows from (2.14).

Analysis of the results reported in Ref. 35 also shows that molecular ions are produced mostly in a time that is much longer than the duration of the exciting laser pulse ($\tau=3$ ns), whilst atomic ions are formed during the pulse itself. This suggests that there is an additional channel for the production of atomic ions in situations[35] such as stepwise ionization or ionization induced by radiation:

$$X^{**}+X^{**}+h\nu\rightarrow X^{+}+X+e. \tag{5.4}$$

Under similar conditions,[125] process (5.4) can dominate the production of atomic ions when the rate constant for (5.4) is of the order of 10^{-16} $W\cdot cm^5\cdot s^{-1}$.

A theoretical estimate was obtained in Ref. 42 for the rate constant for Penning ionization in collisions between 11^2P atoms of rubidium (cf. Sec. 2), namely, 2×10^{-8} $cm^3\cdot s^{-1}$ which is close to the AI rate constant and lower by a factor of 5 than the PI rate constant ($T=60$ K) calculated in Ref. 35 by the Monte Carlo method.

Advances in high-resolution electron spectroscopy and laser technology have given us the electron spectra from reactions (2.7) and (2.8) (Ref. 126). An interesting result was obtained on the role of the following intermediate excited configurations in (2.8):

$$X^{**}(nl)+X^{**}(n'l')\rightarrow X^{+}+X+e, \tag{5.5}$$

$$X^{**}(nl)+X^{**}(n'l')\rightarrow X^{+}X^{*}+e. \tag{5.6}$$

According to Ref. 126, the cross section for (5.6) is greater by a factor of 6–15 than for (5.5).

5.3. Production of a pair of positive and negative ions

Energy considerations show that with increasing n ($1/2n^2<E_a$, where E_a is the electron affinity energy), the formation of the ion pair in (2.6) can occur only if we retain the third term which crosses the original covalent and ionic terms by analogy with the AI (5.3) of excited helium atoms.

Processes such as (2.6) were investigated in Ref. 127 in the case of the reaction $Rb(nl)+Rb(5^2S)\rightarrow Rb^{+}+Rb^{-}$, $T=543$ K and for levels lying both above (5^2D, 7^2S, 6^2D, 8^2S) and below (7^2D, 9^2S, 8^2D, 10^2S) the potential curve of the system $Rb^{+}Rb^{-}$ for $R\rightarrow\infty$. According to these data, the rate constant for the process rises from 10^{-14} $cm^3\cdot s^{-1}$ for the 5^2D level to 10^{-10} $cm^3\cdot s^{-1}$ for the 6^2D level. For the 5^2D and 7^2S levels, the Landau-Zener theory is in good agreement with experiment (Table V).

The formation of negative ions in collisions between Rydberg atoms ($n=7$–40) was investigated experimentally in Ref. 124. For $n\geqslant20$, the main channel for the production of negative sodium ions was found to be (2.9). The results obtained were found to be in good agreement with theoretical calculations[34] extrapolated to thermal collision energies (cross sections of the order of 10^{-13} cm^2). An unsuccessful attempt was also made in Ref. 124 to estimate the cross section for the radiative process

$$Na^{**}+Na^{**}\rightarrow Na^{+}+Na^{-}+h\nu, \tag{5.7}$$

which can be identified with the radiative attachment of a highly-excited quasifree Rydberg electron. The production of negative ions in binary collisions between Rydberg atoms was also observed in Ref. 35. The specificity of the Rydberg state is that its components, namely, the ion core and the weakly-bound free electron, can determine the character of the collision process. The ion core governs the character of the diffusion of the HEA and the scattering of electrons with orbital kinetic energy of the order of 0.001 eV manifests itself in collisions between HEAs and molecules.

TABLE VI. Rate constants for chemi-ionization at thermal energies in collisions of sodium atoms in $4^2D_{5/2}$ and $5^2S_{1/2}$ states on the one hand and halogen-containing molecules, $T=600$ K (Refs. 6 and 128).

Atom, molecule	k, 10^{-10} cm^3 s^{-1}	σ, 10^{-13} cm^2	Resulting negative ions
1. Na(4^2D), SF_6	2,8 ± 0,8	1,6*) 4,6	SF_6
2. Na(4^2D), CH_3Br	0,35 ± 0,1	8,4 2,5	Br^-
3. Na(4^2D), CCl_2F_2	0,54 ± 0,2	2,8	23 % Cl_2^- + + 77 % Cl^- or F_2^-
4. Na(4^2D), C_6F_6	0,08 ± 0,03	$1{,}2\cdot10^{-4}$	$C_6F_6^-$
5. Na(4^2D), C_6F_5H	0,18 ± 0,06	$2{,}7\cdot10^{-4}$	—
6. Na(4^2D), CH_3I	2,1 ± 0,6	—	I^-
7. Na(5^2S), O_2	0,13 ± 0,04	—	O_2^-
8. Na(5^2S), SF_6	0,16 ± 0,05	—	SF_6^-

*) Reactions 1-4 and 7 are endothermic so that the value is based on E_a used in the analysis of measured reaction rates.

Table VI lists the ionization rate constants and cross sections for collisions between $4^2D_{5/2}(E_i^* = 0.86$ eV) and $5^2S_{1/2}(E_i^* = 1.02$ eV) sodium atoms, on the one hand, and halogen-containing molecules for sodium beam-source temperature $T=600$ K, on the other. For exothermic reactions with $\Delta E>0$, the inital and final potential energy curves do not cross, which reduces the electron transfer probability and, consequently, the reaction cross section as well (Table VI). This conclusion is consistent with measurements[29] of the cross sections for isothermic ionization reactions on excited 4^2S lithium atoms in collisions with NO_2 molecules ($\sigma=2\times10^{-19}$ cm^2), Cl_2 molecules ($\sigma=2\times10^{-17}$ cm^2), and F_2 molecules (2×10^{-16} cm^2).

The cross section for the production of an ion pair was found in Ref. 130 to be a function of the degree of vibrational excitation of halogen-containing molecules colliding with fast alkali-metal atoms. The same effect was observed in Ref. 6 in thermal collisions. In the latter case, the effect of vibrational excitation on the electron-transfer probability may have been due to a number of factors such as a reduction in the reaction energy threshold, a change in the vertical electron affinity energy, and so on. These results are of undoubted practical interest for the detection of vibrationally-excited molecules. For halogen-containing molecules, characterized by high rate constants ($k\sim10^{-7}$ cm^3 s^{-1}, SF_6), the negative-ion yield in thermal collisions with HEAs is determined by the HEA attachment probability. This follows from the theory and is confirmed by measurements of the ionization rate constants for HEAs with $n=20$–100 in collisions with halogenides. For example, the chemi-ionization rates have been measured[78] for collisions between rubidium HEAs ($n=38$–106) and SF_6 molecules. In the impulse approximation, the cross section for colisions between HEAs and target molecules is determined by the HEA scattering cross section at energies of the order of 0.001 eV on halogen-containing molecules. For the $X^{**}+SF_6\rightarrow X^++SF_6^-$ reaction, the cross section is inversely proportional to the orbital velocity of the electron in its highly excited state: $\sigma(v)=(4.2\pm1.0)\times10^{-7}/v$. Since the Rydberg states of all atoms are similar, an analogous result is also obtained for xenon HEAs. As the principal quantum number is varied in the range $n=23$–106, the HEA chemi-ionization rate constant for collisions with SF_6 is found to lie in the range 4×10^{-7}–4.5×10^{-7} cm^3 s^{-1} and is practically independent of n. We note that, by considering a highly-excited and a ground-state hydrogen atom, it was shown in Ref. 131 that the cross section for the ionization of an HEA colliding with a neutral atomic particle should be equal to the elastic scattering cross section of the particle for a weakly-bound electron.

In a recent paper[132] on the ionization of n^2P Rydberg atoms of sodium ($n=24$–32) in collisions with SF_6 molecules, it was found that there was reasonable agreement with previously published data for Xe(nF) ($n=25$–40), Rb(nS) ($n=49$–62), and Rb(nD) ($n=38$–106). An interesting new result is that there is a systematic discrepancy between the rate constants measured in experiments on the attachment of slow electrons to molecules, on the one hand, and the chemi-ionization measurements on HEAs, on the other. For other complex molecules, k either increases with increasing n (CCl_4, CCl_3F, CH_3I) or decreases (C_7F_{14}) (see, for example, Ref. 2). The detailed dependence of σ on n is determined by the properties of the scattering of ultraslow HEAs by molecules. Associative and Penning ionization in collisions between potassium atoms in metastable autoionizing states (MASs) and D_2, NO, N_2, CO, CO_2, N_2O, H_2O, and H_2S molecules was investigated semiquantitatively in Ref. 133. According to these data, the Penning ionization cross sections are of the order of 10^{-15} cm^2. The complex ions KHe^+, KNe^+, KKr^+, and KXe^+ have also been recorded in collisions between MASs and inert-gas atoms. As n decreases, the quasidiscrete character of the energy levels of the excited electron becomes clearer and the chemi-ionization can no longer be correctly described in terms of the pure impulse mechanism. Finally, the harpoon model of the reaction, based on an analysis of specific quasimolecular terms, becomes valid for the lowest-lying excited states. These examples clearly illustrate the basic diffculties encountered when attempts are made to construct universal models of chemi-ionization in a wide range of values of n even for a given atom. The high rate constants for the production of the SF_6^- ions are due to the fact that this ion is appears in a long-lived excited state with lifetime $\tau>0.001$ s. A different situation arises for intermediate states in collisions between the alkali metals and O_2 molecules: the lifetime of the resulting O_2^{-*} ion is very short ($\tau\approx10^{-9}$ s) and, in the absence of a stabilizing mechanism, we have electron autodetachment.[134] The interaction with the ion core of the Rydberg atom can serve as a stabilizing factor. If stabili-

zation is less effective for smaller n then, in contrast to the above case of collisions with SF_6, the rate constant for O_2 should decrease with n. This may be the explanation of the low value of k (10^{-12} cm^3 s^{-1}) and the reduction in k with increasing n ($8 \leqslant n \leqslant 12$) reported in Ref. 135. When the colliding particles are suitably chosen, chemi-ionization is an effective method of ionizing an excited medium. Molecules with high electron affinity (for example, UF_6, $E_a = 4.9$ eV) can thus be used in the selective excitation of atoms by visible radiation, which is of interest, for example, for laser separation of isotopes.[7]

Ionization cross sections for HEAs colliding with dipolar molecules such as H_2O, NH_3, SO_2, C_2H_5OH, and CH_3NO_2 are given in Ref. 2. For $n > 30$, the corresponding rate constants tend to their asymptotic limit (10^{-6} cm^3 s^{-1}, H_2O, NH_3). Experimental data on ionization in collisions between Rydberg atoms and polar molecules, or molecules with positive electron affinities, can be found in Ref. 135.

The above review of existing data on chemi-ionization rate constants at thermal energies shows that the values of these constants for nonthreshold reactions reach values of the order of 10^{-6}–10^{-10} cm^3 s^{-1}. They constitute an effective channel for the ionization of excited atoms, which in turn offers the prospect of practical applications. Modern beam techniques, used in combination with laser excitation of atoms and molecules, provide data on electron spectra, autoionization widths, and the mass spectrum of reaction products that had previously been inaccessible to many research groups. These data are particularly valuable because chemi-ionization theory is, on the whole, still in the development stage.

6. SECONDARY PROCESSES IN CHEMI-IONIZATION EXPERIMENTS

Modern tuneable dye lasers can be used for the resonant optical excitation of the atoms of virtually all the elements in the periodic table. This means that researchers can now design chemi-ionization experiments employing selective laser excitation techniques. However, the introduction of these fundamentally new experimental facilities has been accompanied by specific new effects than have hindered such experiments. A reduction in molecular-ion yield of the AI channel (2.4) with increasing laser-beam power has been observed in the laser excitation of the Rydberg states of strontium [reaction (2.4); Ref. 136], lithium,[35] and rubidium [reaction (2.7); Ref. 125]. According to Refs. 35 and 136, the observed effect is due to the production of laser photoplasma and the destruction of selectively excited states by electrom impact. We recall that an analogous result was observed in the AI channel (2.2) in Ref. 137 which was the first to report a new physical phenomenon, namely, the production of current-free photoresonant plasma (Fig. 13). The theory of the resonant optical discharge[138,139] was subsequently developed for the conditions prevailing under laser excitation of an absorbing medium consisting of alkali-metal atoms. Calculations performed within the framework of the theory show that for alkali-metal vapor with $10^{15} \leqslant N_0 \leqslant 10^{17}$ cm^{-3} and

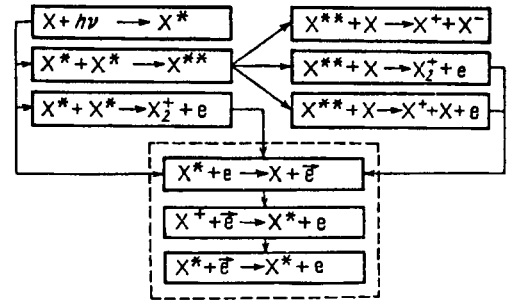

FIG. 13. Scheme illustrating possible mechanisms for the evolution of photoplasma during absorption of resonant radiation.

laser illumination of $10^5 \leqslant I \leqslant 10^7$ W cm^{-2} (line width about 0.05 nm), AI is the dominant source of primary electrons in K, Rb, Cs, and Na ($I \leqslant 10^6$ W·cm^{-2}). In the most frequently investigated case, i.e., laser excited sodium vapor, such measurements were started abroad in the 70s and 80s (Ref. 140), and the contribution of AI via reaction (2.2) to the overall ionization balance was found to reach up to 20%.

As the illuminating intensity increases, further ion and electron producing channels come into play. They include stepwise ionization, laser-induced collisional ionization, and also photodestruction of ion clusters.

An increase in the excited-atom concentration (the usual objective in chemi-ionization experiments), produced by higher laser power, thus necessarily leads to a loss of selectivity in primary excitation and the photodestruction of the byproducts of these reactions. In particular, this means that selective optical (laser) excitation becomes unpromising as a means of producing population inversion in gaseous media.[141]

When the resonant transition becomes saturated (in alkali-metal vapor), the heating of electrons by collisions of the second kind becomes significant beginning with concentrations of ground-state atoms $N_0 \leqslant 2 \times 10^{13}$ cm^{-3}. This imposes restrictions on I and N_0 in experiments concerned with elementary processes that involve selectively excited atoms. They are: $I \leqslant 100$ W·cm^{-2}($N_0 \geqslant 10^{13}$ cm^3) and the use of the gas cell.[142]

The second process that significantly influences the ionization kinetics under selective optical excitation of low-lying atomic states is the so-called energy pooling process.[142–147] As the primary excitation energy increases in collisions of this kind, the excited atomic system enters the region of high effective principal quantum numbers that correspond to the maximum of the function $k(n_{\text{eff}})$ (see Fig. 10).

It was noted in laser excitation experiments (see, for example, Ref. 148) that the excited-state lifetime can be much shorter than the radiative lifetime (by an order of magnitude or more). This is due to the specific laser process of cascade superradiance that takes place under high laser power densities. The cascade de-excitation of high-lying levels by superradiance (spontaneous collective emis-

TABLE VII. Cascade superradiance parameters for the laser-excited $7^2P_{1/2}$ level of potassium[126]

Transition	λ, nm	Transition oscillator strength	Threshold values of N^*L, cm^{-2}
$7\,^2P_{1/2}-7\,^2S_{1/2}$	12,6	0,79	$5{,}4\cdot10^9$
$7\,^2S_{1/2}-6\,^2P_{1/2,3/2}$	7,9	1,37	$5{,}1\cdot10^9$
$7\,^2P_{1/2}-5\,^2D_{3/2}$	11,3	0,76	$6{,}3\cdot10^9$
$5\,^2D_{3/2}-6\,^2P_{1/2,3/2}$	8,5	0,92	$7{,}1\cdot10^9$

sion) arises when the characteristic time of the process, t_R, becomes much shorter than the "dephasing" time[149]

$$t_R=\frac{8\pi}{N^*L\lambda^2A}, \tag{6.1}$$

where N^* is the concentration of excited atoms occupying the upper level, L is a typical linear dimension of the active region in which superradiance can be localized, and A is the radiative transition probability.

For the relatively low densities of ground-state atoms that are generally common in chemi-ionization experiments, the main process responsible for "dephasing" is the Doppler effect for which $t_{ph}=\pi(\Delta\nu^D)^{1/2}$. It is readily seen that $t_{ph}/t_R\sim\lambda^2$, from which it follows that cascade superradiance effects are most likely to be observed in infrared transitions.

As an illustration, Table VII lists the threshold densities of excited 7^2P potassium atoms that correspond to the onset of the superradiance process: $N_0=10^{14}$ cm^3, laser pulse length 10 ns, $L=11.6$ cm pulse length 8 ns, delay relative to the exciting radiation 16.5 ns.

The AI quantum yield, i.e., the number of charged particles produced per absorbed photon in (2.4), is reduced by 20 and 100% by the superradiance effect when the threshold values of N^* are exceeded by a factor of 10 and 100, respectively. As I increases and the number of ground-state atoms in the reaction zone decreases, photoionization processes with appreciable cross sections begin to dominate the situation. The same effect should be observed when the spectral linewidth of the exciting laser pulse increases. In the papers cited above, photoionization by laser light was the main source of primary electrons under the conditions reported in Ref. 136. Since, for Rydberg states, the maximum photoionization cross section corresponds to the infrared range, experiments with Rydberg atoms having $18\leqslant n\leqslant35$ exhibit the effects of photoionization by blackbody radiation corresponding to the temperature of the walls of the vapor-filled cell[150] ($T=500$ K).

The competition between two-photon ionization and Penning ionization stimulated by radiation under laser excitation of the 3^2P levels of sodium was considered in Ref. 44. In this case, photoionization becomes the dominant

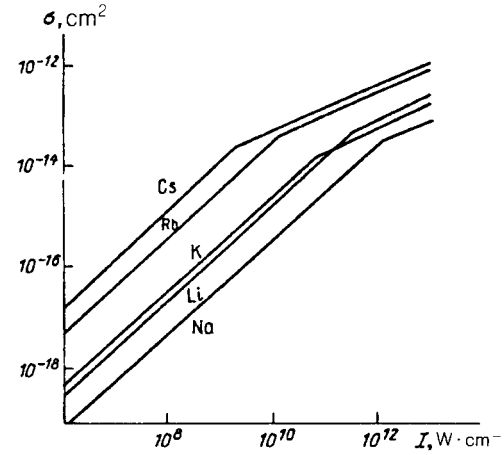

FIG. 14. Cross section for Penning ionization stimulated by radiation.[44]

ionization channel, but only for radiation power densities in excess of 10^7 W/cm^2. When an absorbing medium (alkali-metal vapor) is excited by laser radiation whose wavelength is different from the resonant-transition wavelengths, the atoms may display the effects of the photoionization of cluster formations present in the form of microimpurities, e.g., three-photon ionization of N_2 molecules under laser illumination of sodium vapor.[151]

It is useful to note that laser experiments concerned with ionization phenomena for $I\geqslant10^5$ W·cm^{-2} have not revealed any saturation effects in the charged-particle current[95] although optical-signal saturation, i.e., resonant fluorescence, is seen for much lower illumination power densities (see, for example, Refs. 95 and 152). This means that the dynamics of the system of colliding atoms may change significantly in the laser radiation field, and laser-induced associative and Penning ionization processes may come into play. The measured cross section s for such processes with $I\approx10^6$ W·cm^{-2} are 3×10^{-19} cm^2 and 5×10^{-19} cm^2 for Na (Ref. 95) and Li (Ref. 153), respectively, and are in reasonable agreement with calculations[44] (Fig. 14). When the exciting laser pulse length is comparable with the lifetime of the excited states, one begins to see the effects of the photodissociation of molecular ions produced in AI channels. Thus, in crossed-beam experiments using sodium beams ($N_0=10^9$ cm^{-3}), the Na_2^+ ions produced according to Ref. 152 for $I<6\times10^4$ W·cm^{-2} in reaction (2.2) undergo partial photodissociation during the laser pulse. Since molecular ions produced in dimer AI and photoionization channels have different vibrational excitation, the photodissociation cross section s are correspondingly different.[154]

7. CHEMI-IONIZATION IN MODERN APPLICATIONS OF THE PHYSICS AND CHEMISTRY OF LOW-TEMPERATURE PLASMAS

The above ionization processes in thermal collisions between heavy particles produce a change in the charged-particle balance in low-temperature plasmas with ioniza-

tional or recombinational departure from equilibrium. Even simple qualitative considerations show that the chemi-ionization processes should have maximum influence on ionization kinetics in the case of alkali-metal atoms or atoms with a similar structure of excited-state terms. For such systems with a relatively uniform sequence of energy levels, excitation to to a resonant level does not necessarily mean that the excited electron will immediately enter the continuum, i.e., the bottleneck usually lies higher in such cases, and the effective 'sink' consisting of chemi-ionization from low-lying levels can significantly affect the resultant ionization rate. Conversely, for inert-gas atoms, the ionization rate is practically always limited by the rate of excitation of low-lying states, followed by their immediate ionization in electron-atom collisions.

It used to be believed that, in low-temperature plasmas, chemi-ionization played a significant part only in the early stages of ionization, i.e., in gas breakdown, in shock waves, and so on. Dissociative recombination processes reduce the contribution of chemi-ionization to ionization kinetics. However, there is a situation in which chemi-ionization (with the formation of a molecular ion) is not accompanied by the reverse recombination process. Indeed, the thermal dissociation of molecular ions proceeds effectively when the temperature of the normal component of the alkali-metal plasma is $T \geqslant 1000$ K, and the role of these ions in recombination kinetics declines.[155]

Chemi-ionization processes that are effective in thermal collisions of atoms and molecules occur mostly at the expense of the internal excitation energy. It follows that chemi-ionization can play a very significant role in low-temperature plasmas in which the potential energy stored in excited states exceeds the energy of the electron gas by a few orders of magnitude. The clearest examples of this are provided by cryogenic plasmas, afterglow plasmas, and photoplasmas.

There have been recent suggestions that the chemi-ionization reaction could be used in a number of nontraditional applications of plasma physics. For example, the photoprocess of chemi-ionization of impurity atoms can be regarded as an alternative to photoionization as an efficient source of primary charged particles in the preionization stage of a discharge in a high-pressure molecular gas.[157] Other proposed applications that can be introduced here include the detection of vibrationally-excited molecules, laser separation of isotopes, and laser optogalvanic spectroscopy based on chemi-ionization.[6]

We now present (following Ref. 157) specific examples that illustrate the role of chemi-ionization in the kinetics of low-temperature nonequilibrium plasmas.

Plasmas with ionizational departure from equilibrium:

—significant contribution of chemi-ionization reactions to ionization in a sufficiently wide range of parameters of alkali-metal plasmas in thermoemissive energy converters

—production of population inversion in discharges occuring in mixtures of inert gases and metal vapors.

Plasmas with recombinational departure from equilibrium:

—effect of chemi-ionization on the rate of change in the electron concentration and temperature in the afterglow of weakly-ionized inert-gas plasma

—enrichment of the electron energy distribution with fast electrons in afterglow plasmas, the resulting increase in the contribution of stepwise processes to the population of excited states, and the consequent possible change in the character of departure from equilibrium

—formation of an anomalous discontinuity in potential near the wall due to fast electrons released by chemi-ionization in current-free plasma

—cleanup of low-lying laser levels by ionization of impurities in the chemi-ionization channel.

Recent advances in the control of the properties of atomic beams and the development of laser systems for the cooling and confinement of cold ions and neutral atoms have led to the initiation of chemi-ionization experiments in which the relative kinetic energy of the particles is equivalent to temperatures between a few dozen of degrees Kelvin and a few millikelvins or less. The results of these early experiments with cold atoms demonstrate the considerable promise of this approach to the physics of collisions involving atoms, molecules, and clusters at cryogenic temperatures. It is clear that chemi-ionization is a very significant process in cryogenic plasmas with record concentrations of metastable atoms.

In conclusion, we consider the possible utilization of chemi-ionization in resonant ionization spectroscopy. This phrase refers to the set of methods and processes dedicated to the solution of specific applied problems such as the detection of individual atoms and molecules or the laser separation of isotopes. The method relies on the conversion of resonantly excited particles into atomic or molecular ions, including conversion via the chemi-ionization channel. Practically the same mechanisms of resonant ionization spectroscopy in low-temperature plasmas are called optogalvanic and optoelectric effects that are seen as changes in ionizational, electric, and vibrational properties of plasmas.[158] Optogalvanic techniques are being used to obtain information about the products of plasmochemical reactions; they are also used for spectro-analytic purposes and as detectors of laser radiation. Another phenomenon that belongs here is the specific case of light-induced current in a rarefied gas in which absorption of monochromatic radiation and the Doppler effect result in the production of excited particles with monodirectional velocities. The optogalvanic effect (light-induced current) can then be observed without having to apply a potential difference to the vapor in the discharge gap.[159]

8. CONCLUSION

We have surveyed some of the chemi-ionization studies performed during the last twenty years, many of them by Russian physicists. It is clear from this review that the last two decades were a period of intense activity in the study of chemi-ionization in thermal collisions of atoms and mole-

cules. The results obtained demonstrate the extensive and often unique possibilities of this new branch of the physics of atom-molecule collisions and the associated considerable range of practical applications. All experience gained to date suggests that attempts to construct a modern theory of physical phenomena that are of immediate interest in technical physics and chemistry must fail unless we take into account ionization by collisions with excited heavy particles. Nor is there any doubt that new experiments exploiting latest advances in atomic-beam technology and laser cooling and confienment systems for excited atoms, will lead to new discoveries in the near future. In this sense, chemi-ionization studies have a very promising future.

My objective in presenting this review will be largely fulfilled if I succeed in attracting the attention of physicists—especially young physicists planning their future careers in science—to the questions discussed above.

I am greatly indebted to V. M. Borodin for helpful discussions of the theoretical aspects of chemi-ionization.

[1] A. N. Klyucharev, Khim Plazmy, edited by B. M. Smirnov, Energoatomizdat, M., No. 7, 109 (1980).
[2] B. M. Smirnov, *Excited Atoms* [in Russian], Energoatomizdat, M., 1982.
[3] A. N. Klyucharev, and M. L. Yanson, *Elementary Processes in Alkali-Metal Plasmas* [in Russian], Energoatomizdat, M., 1988.
[4] A. N. Klucharev and V. Vujnovic, Phys. Rept. 185, 55 (1990).
[5] F. Mohler and C. Boeckner, J. Res. Nat. Bur. Standards, Sec. A **5**, 399 (1930).
[6] I. M. Beterov, V. L. Kurochkin, and N. V. Fateev, Khim. Fizika **1**, 957 (1982).
[7] I. M. Beterov and N. V. Fateev, Khim. Plazmy, edited by B. M. Smirnov, Energoatomizdat, M., no. **13**, 40 (1987).
[8] V. M. Borodin, V. Vuĭnovich, B. V. Dobrolezh *et al.*, *Ionization with Atomic Excitation* [in Russian], edited by N. P. Penkin and A. N. Klyucharev, LGU, L., p. 4, 1989.
[9] W. H. Miller, J. Chem. Phys. **52**, 3563 (1970).
[10] H. I. Nukamura, Phys. Soc. Jpn. **31**, 574 (1971).
[11] R. S. Berry and S. E. Nielsen, Phys. Rev. A **1**, 383 (1970).
[12] R. S. Berry and S. E. Nielsen, Phys. Rev. A **1**, 395 (1970).
[13] R. S. Berry and S. E. Nielsen, Phys. Rev. A **4**, 865 (1971).
[14] E. A. Duman and I. P. Shmatov, Zh. Eksp. Teor. Fiz. **79**, 2116 (1980) [Sov. Phys. JETP **51**, 1061 (80)].
[15] A. Mihajlov and R. Ianev, Phys. Rev. A **21**, 819 (1980).
[16] A. Z. Devdariani, A. N. Klyucharev, N. P. Penkin, and Yu. N. Sebyakin, Opt. Spektrosk. **64**, 706 (1988) [Opt. Spectrosc. (USSR) **64**, 425 (1988)].
[17] R. G. Newton, *Scattering Theory of Waves and Particles*, Springer-Verlag, N.Y., 1982 [Russ. transl. of earlier edition, Mir, M., 1969].
[18] G. K. Ivanov and G. V. Golubkov, Phys. Chem. Phys. **107**, 261 (1984).
[19] A. K. Kazanskiĭ, Khim. Fiz. **4**, 295 (1985).
[20] R. K. Ianev and P. S. Krstic, J. Phys. B **19**, 3695 (1986).
[21] G. K. Golubkov and G. V. Ivanov, J. Phys. B **21**, 2049 (1988).
[22] U. Fano, Phys. Rev. A **2**, 353 (1970).
[23] U. Fano, J. Opt. Soc. Am. **65**, 979 (1975).
[24] G. K. Golubkov and G. V. Ivanov, Zh. Eksp. Teor. Fiz. **8**, 132 (1981) [Sov. Phys. JETP **54**, 64 (1981)].
[25] G. K. Golubkov and G. V. Ivanov, Khim. Fiz. **6**, 729 (1982).
[26] G. K. Golubkov and G. V. Ivanov, Z. Phys. D **1**, 199 (1986).
[27] A. Z. Devdariani, Opt. Spektrosk. **47**, 106 (1979) [Opt. Spectrosc. (USSR) **47**, 58 (1979)].
[28] B. M. Smirnov, Usp. Fiz. Nauk **133**, 569 (1981) [Sov. Phys. Usp. **24**, 251 (1981)].
[29] B. M. Smirnov and A. A. Mikhaĭlov, Opt. Spektrosk. **30**, 964 (1971).
[30] A. Z. Devdariani, A. N. Klyucharev, A. V. Lazarenko, V. A. Sheverev, Pis'ma Zh. Tekh. Fiz. **4**, 1013 (1978) [Sov. Tech. Phys. Lett. **4**, 408 (1978)].
[31] A. A. Mihajlov and R. K. Ianev, J. Phys. B **14**, 1639 (1981).
[32] V. S. Lebedev and V. S. Marchenko, Khim. Fiz. **3**, 210 (1984).
[33] M. R. Flannery, Ann. Phys. **61**, 465 (1970).
[34] R. E. Olson, Phys. Rev. Lett. **43**, 126 (1979).
[35] M. W. McGeoch, R. E. Schlier, and G. K. Chawla, Phys. Rev. Lett. **61**, 2088 (1988).
[36] B. M. Smirnov, and O. V. Firsov, Pis'ma Zh. Eksp. Teor. Fiz. **2**, 478 (1965).
[37] K. Katsuura, J. Chem. Phys. **42**, 3771 (1965).
[38] T. Watanabe and K. Katsuura, J. Chem. Phys. **47**, 800 (1967).
[39] A. Z. Devdariani, V. N. Ostrovskiĭ, and Yu. N. Sebyakin, Zh. Eksp. Teor. Fiz. **71**, 900 (1976).
[40] A. Z. Devdariani, V. N. Ostrovskiĭ, and Yu. N. Sebyakin, Zh. Eksp. Teor. Fiz. **76**, 529 (1979) [Sov. Phys. JETP **49**, 266 (1979)].
[41] A. Z. Devdariani, A. L. Zagrebin, and Yu. N. Sebyakin, *Ionization with the Participation of Excited Atoms* [in Russian], edited by N. P. Penkin and A. N. Klyucharev, LGU, L., p. 70, 1989.
[42] V. M. Borodin, B. V. Dobrolezh, A. N. Klyucharev, and A. B. Tsyganov, Abstracts of Papers Presented to the Eighth Conf. on the Physics of Low-Temperature Plasmas [in Russian], Minsl, 1991, vol. **1**, p. 13.
[43] P. L. Gould, P. D. Lett, P. S. Julienne *et al.* Phys. Rev. Lett. **60**, 788 (1988).
[44] S. Geltman, J. Phys. B **21**, L735 (1988).
[45] H. Hartley, A. O. Ponder, E. J. Bowen *et al.* Phil. Mag. **43**, 430 (1922).
[46] A. N. Klyucharev and A. B. Tsyganov, *Exitation and Ionization of Atoms During the Absorption of Light* [in Russian], LGU, L., 1983.
[47] N. N. Bezuglov and A. B. Tsyganov, Opt. Spektrosk. **59**, 195 (1985) [Opt. Spectrosc. (USSR) **59**, 115 (1985)].
[48] J. Huenekens and A. Gallagher, Phys. Rev. A **27**, 771 (1983).
[49] J. Huenekens and A. Gallagher, Phys. Rev. A **28**, 1276 (1983).
[50] W. P. Garver, M. B. Pierce, and J. J. Leventhal, J. Chem. Phys. **77**, 1201 (1982).
[51] N. N. Bezuglov, V. N. Gorshkov, A. L. Osherovich, and G. L. Plekhotkina, Opt. Spektrosk. **53**, 405 (1982) [Opt. Spectrosc. (USSR) **53**, 239 (1982)].
[52] N. N. Bezuglov and V. N. Gorshkov, Opt. Spektrosk. **56**, 1000 (1984) [Opt. Spectrosc. (USSR) **56**, 614 (1984)].
[53] N. N. Bezuglov, Opt. Spektrosk. **85**, 978 (1985).
[54] R. Bonnano, J. Bulmer, and J. Weiner, Phys. Rev. A **28**, 604 (1983).
[55] N. N. Bezuglov, V. M. Borodin, A. N. Klyucharev *et al.*, Khim. Plazmy, edited by B. M. Smirnov, Energoatomizdat, M., no. 13, 3 (1987).
[56] N. N. Bezuglov and A. N. Klyucharev, Zh. Prikl. Spektrosk. **30**, 549 (1979).
[57] N. N. Bezuglov and A. B. Osherovich, Vestnik LGU, no. 16, 44 (1978).
[58] N. N. Bezuglov, V. Vuĭnovich, A. N. Klyucharev, and V. A. Sheverev, Opt. Spektrosk. **66**, 1239 (1989) [Opt. Spectrosc. (USSR) **66**, 721 (1989)].
[59] M. X. Wang and J. Weiner, J. Phys. B **21**, L15 (1988).
[60] M. E. Koch, W. C. Stawalley, and C. B. Collins, Phys. Rev. Lett. **42**, 1052 (1979).
[61] Yu. P. Korchevoĭ, Zh. Eksp. Teor. Fiz. **75**, 1231 (1978) [Sov. Phys. JETP **48**, 620 (1978)].
[62] A. De Iong and F. van der Valk, J. Phys. B **12**, L561 (1979).
[63] N. N. Bezuslov, S. M. Papernov, Zh. L. Shvegzhda *et al.*, Abstracts of Papers presented to the Ninth Conf. on the Physics of Electronic and Atomic Collisions [in Russian], 1984, vol. **1**, p. 139.
[64] L. Barbier and M. Cheret, J. Phys. B **20**, 1229 (1987).
[65] M. X. Wang, M. S. de Vries, J. Keller, and J. Weiner, Phys. Rev. A **32**, 681 (1985).
[66] M. X. Wang, J. Keller, J. Boulmer, and J. Weiner, Phys. Rev. A **35**, 934 (1987).
[67] H. A. Meijer, H. P. van der Meulen, and R. Morgenstern, Z. Phys. D **5**, 299 (1987).
[68] J. Keller, R. Bonanuo, M. X. Wang *et al.*, Phys. Rev. A **23**, 1612 (1986).
[69] J. Lorenzen, H. Hotop, M. W. Ruf *et al.*, Z. Phys A **297**, 19 (1980).
[70] J. G. Kircz, R. Morgenstern, and G. Nienhuis, Phys. Rev. Lett. **48**, 610 (1982).
[71] H. A. J. Meijer, G. M. Heideman, I. V. Hertel *et al.*, Phys. Rev. A **33**, 1421 (1986).
[72] E. W. Rothe, R. Theyunni, G. P. Reck *et al.*, Phys. Rev. A **31**, 1362 (1985).

[73] S. P. Dmitriev, R. A. Zhitnikov, and A. I. Okunevich, Zh. Eksp. Teor. Fiz. **70**, 69 (1976) [Sov. Phys. JETP **43**, 35 (1976)].
[74] D. R. Bates, K. L. Bell, and A. Kingston, Proc. Phys. Soc. **91**, 288 (1967).
[75] Yu. A. Tolmachev, Khim. Plazmy, edited by B. M. Smirnov, Energoatomizdat, M., no. 9, 80 (1982).
[76] N. B. Kolokolov, Khim. Plazmy, edited by B. M. Smirnov, Energoatomizdat, M., no. 12, 56 (1985).
[77] V. S. Egorov, Khim. Plazmy, edited by B. M. Smirnov, Energoatomizdat, M., no. 7, 187 (1980).
[78] B. G. Zollars, C. Higgs, F. Lu *et al.*, Phys. Rev. A **32**, 3330 (1985).
[79] I. M. Beterov, G. L. Vasilenko, I. I. Riabtsev *et al.* Z. Phys. D **7**, 55 (1987).
[80] B. G. Garrison, W. H. Miller, and H. F. Shaefer, J. Chem. Phys. **59**, 3193 (1973).
[81] R. H. Neynaber, Proc. Eleventh Internat. Conf. on the Physics of Electronic and Atomic Collisions, Kyoto, 1979, p. 287.
[82] R. H. Neynaber, C. D. Magnuson, and S. Y. Tang, J. Chem. Phys. **68**, 5112 (1978).
[83] R. Deloche, P. Monchicourt, M. Cheret *et al.* Phys. Rev. A **13**, 1140 (1976).
[84] A. Z. Devdariani, V. I. Demidov, N. B. Kolokolov *et al.*, Zh. Eksp. Teor. Fiz. **84**, 1646 (1983) [Sov. Phys. JETP **57**, 960 (1983)].
[85] V. B. Borisov, V. S. Egorov, and N. A. Ashurbekov, Abstracts of Papers Presented at the Sixth All-Union Conf. on the Physics of Low-Temperature Plasmas [in Russian], L., 1983, vol. 1, p. 20, 1983.
[86] M. W. Muller, A. Mezz, M. W. Ruf *et al.*, Z. Phys. D **21**, 89 (1991).
[87] A. Z. Devdariani, Opt. Spektrosk. **47**, 106 (1979) [Opt. Spectrosc. (USSR) **47**, 58 (1979)].
[88] S. Runge, A. Pesnelle, M. Perdix *et al.*, Phys. Rev. A **32**, 1412 (1985).
[89] H. A. J. Meijer, S. Schohl, and M. W. Muller *et al.*, J. Phys. B **24**, 3621 (1991).
[90] A. Heuriet and F. Masnou-Seeuws, J. Phys. **20**, 671 (1987).
[91] O. Dulieu, A. Giusti-Suzor, and F. Masnou-Seeuws, J. Phys. B **24**, 4391 (1991).
[92] N. N. Bezuglov, A. N. Klucharev, and V. A. Sheverev, J. Phys. B **20**, 2497 (1987).
[93] A. Gallagher, Phys. Rev. A **44**, 4249 (1991).
[94] B. Carre, F. Roussel, P. Breger, and G. Spiess, J. Phys. B **14**, 4271 (1081).
[95] J. Weiner and P. Polak-Dingels, J. Chem. Phys. **74**, 508 (1981).
[96] V. Ju. Sepma, V. A. Sheverev, an A. V. Vujnovic, Lectures at a Seminar at Zagreb on 13–15 p. 64. October 1987.
[97] K. L. Tan and A. von Engel, J. Phys. D **1**, 1877 (1968).
[98] K. L. Bell, A. Dalgarno, and A. E. Kingston, J. Phys. B. **1**, 18 (1968).
[99] P. C. Johnson, M. J. Cooke, and J. E. Allen, J. Phys. D **11**, 1877 (1978).
[100] Yu. A. Tolmachev and D. Fogel', Opt. Spektrosk. **48**, 818 (1980) [Opt. Spectrosc. (USSR) **48**, 451 (1980)].
[101] D. Fogel' and Yu. A. Tolmachev, Opt. Spektrosk. **49**, 824 (1980) [Opt. Spectrosc. (USSR) **49**, 449 (1980)].
[102] G. J. Collins, J. Appl. Phys. **44**, 4633 (1973).
[103] T. Goto, J. Phys. D **15**, 421 (1982).
[104] M. Ianson, J. Klavins, and v. Groushevskii, Abstracts of Fourth European Conf. on Atomic and Molecular Physics, Riga, vol. **16B**, part 2, p. 359 (1992).
[105] D. I. Slovetskiĭ, *Chemical-Reaction Mechanisms in Nonequilibrium Plasmas* [in Russian], Nauka, M., 1980.
[106] L. S. Polak, P. A. Sergeev, and D. I. Slovetskiĭ, Teplofiz. Vys. Temp. **15**, 15 (1977).
[107] D. G. Stoyanov, *Abstract of Thesis* [in Russian], L., 1989.
[108] P. L. Deleon and I. W. Rich, Chem. Phys. **107**, 283 (1986).
[109] A. V. Berdyshev, I. V. Kochetov, and A. P. Napartovich, Fizika Plazmy **14**, 741 (1988).
[110] G. M. Grigoryan, Y. Z. Lonikh, I. V. Kochetov, and V. G. Pevgov, J. Phys. D **25**, 1064 (1992).
[111] M. V. McCusker, L. L. Hatfield, and G. K. Walters, Phys. Rev. A **5**, 117 (1972).
[112] P. J. Keliher, R. E. Cleason, and G. K. Walters, Phys. Rev. A **11**, 1279 (1975).
[113] L. D. Schearer, Phys. Rev. A **10**, 1380 (1974).
[114] H. Morgner, Invited Papers of XIII ICPEAC, p. 451 Berlin, 1983.
[115] B. C. Johnson and M. X. Wang, J. Phys. B **21**, 2599 (1988).
[116] L. Barbier, A. Pesnelle, and M. Cheret, J. Phys. B **28**, 1249 (1987).
[117] H. F. Wellenstein and W. W. Robertson, J. Chem. Phys. **56**, 1077 (1972)
[118] S. Runge, A. Preselle, M. Perdix *et al.*, Phys. Rev. A **32**, 1412 (1985).
[119] J. S. Cohen, Phys. Rev. A **13**, 86 (1976).
[120] A. Henriet and F. Masnou-Seeuws, J. Phys. B **23**, 219 (1990).
[121] R. E. Olson, J. Phys. B **12**, L109 (1979).
[122] J. Weiner and J. Boulmer, J. Phys. B **19**, 599 (1986).
[123] L. P. Presnyakov and A. D. Ulantsev, Kratkie Soobshcheniya po Fizike FIAN, no. 1, 38 (1984).
[124] M. Ciocca, M. Allegrini, E. Arimondo *et al.*, Phys. Rev. Lett. **56**, 704 (1986).
[125] B. V. Dobrolezh, A. N. Klucharev, and A. B. Tsyganov, European Conf. on Atomic and Molecular Physics, Riga, vol. 16B, part 1, p. 102 (1992).
[126] H. A. J. Meijer, H. Dengel, S. Schohl *et al.*, European Conf. on Atomic and Molecular Physics, Riga, vol. 16B, part 2, p. 353 (1992).
[127] L. Barbier, M. T. Djerad, and M. Cheret, Phys. Rev. A **34**, 2710 (1986).
[128] I. M. Beterov and N. V. Fateev, Abstracts of Papers Presented to the Sixth All-Union Conference on the Physics of Low-Temperature Plasmas [in Russian], Leningrad, p. 31, 1983.
[129] G. P. Reck, B. P. Mathur, and E. W. Rothe, J. Chem. Phys. **66**, 3847 (1977).
[130] A. M. C. Moutinho, I. A. Aten, and A. Los, Physica **53**, 471 (1971).
[131] S. T. Butler and R. M. May, Phys. Rev. A **137**, 10 (1965).
[132] I. M. Beterov, G. L. Vasilenko, B. M. Smirnov, and N. V. Fateev, Zh. Eksp. Teor. Fiz. **93**, 31 (1987) [Sov. Phys. JETP **66**, 17 (1987)].
[133] V. N. Slavik, S. E. Kupryanov, and A. A. Perov, Abstracts of Papers Presented to the Seventh All-Union Conference on the Physics of Electronic and Atomic Collisions [in Russian], Petrozavodsk, vol. 2, p. 108, 1978.
[134] C. W. Walter, B. C. Zollars, C. B. Johnson *et al.*, Phys. Rev. A **34**, 4431 (1986).
[135] F. B. Dunning and R. F. Stebbings, *Rydberg States of Atoms and Molecules*, Cambridge University Press, Cambridge, 1983 [Russ. transl., Mir, M., 1985].
[136] E. F. Worden and J. A. Paisner, Opt. Lett. **3**, 156 (1978).
[137] N. D. Morgulis, Yu. P. Korchevoĭ, and A. M. Przhonskiĭ, Zh. Eksp. Teor. Fiz. **53**, 417 (1967).
[138] R. M. Measures and P. G. Cardinal, Phys. Rev. A **23**, 804 (1981).
[139] T. Stacewicz and G. Topulos, Physica Scripta **38**, 560 (1988).
[140] T. B. Lucatorto and T. J. McIlrath, Appl. Optics **19**, 3948 (1980)
[141] A. N. Klyucharev and V. Yu. Sepman, Opt. Spektrosk. **34**, 425 (1973).
[142] A. Kopystynska and L. Moi, Phys. Rept. **92**, 135 (1982).
[143] Zh. I. Shvegzhda, S. M. Papernov, and M. L. Ianson, Phys. Chem. Phys. **101**, 187 (1983).
[144] J. Huennekens and A. Gallagher, Phys. Rev. A **27**, 771 (1983).
[145] P. Kowalczyk, Phys. Chem. Phys. **68**, 203 (1979).
[146] V. M. Borodin and I. V. Komarov, Opt. Spektrosk. **36**, 250 (1974).
[147] A. Kopystynska, Physica Scripta **36**, 288 (1987).
[148] V. Svedas and Z. Kaprionis, Appl. Opt. **52**, 385 (1991).
[149] I. C. McGillivray and M. S. Feld, Phys. Rev. A **14**, 1169 (1976).
[150] C. E. Burkhard, R. L. Corey, W. P. Garver, and J. J. Leventhal, Phys. Rev. **34**, 80 (1986).
[151] C. E. Burkhard, W. P. Garver, and J. J. Leventhal, Phys. Rev. A **31**, 505 (1985).
[152] M. Allegrini, G. Alzetta, A. Kopystynska, and L. Moi, Opt. Comm. **19**, 96 (1976).
[153] A. von Hellfeld, J. Caddick, and J. Weiner, Phys. Rev. Lett. **40**, 1369 (1978).
[154] F. Roussel, B. Carre, P. Breger, and G. Spiess, J. Phys. B **16**, 1749 (1983)
[155] A. A. Kudryavtsev, Teplofiz. Vys. Temp. **25**, 1041 (1987).
[156] A. N. Klyucharev, V. A. Rodichkin, V. Yu. Sepman, and V. A. Sheverev, Pis'ma Zh. Tekh. Fiz. **10**, 277 (1984) [Sov. Tech. Phys. Lett. **10**, 116 (1984)].
[157] N. B. Kolokolov and A. A. Kudryavtsev, Khim. Plazmy, edited by B. M. Smirnov, Energoatomizdat, M., No. 15, 127 (1989),
[158] I. M. Beterov, A. V. Eletskiĭ, and B. M. Smirnov, Usp. Fiz. Nauk **156**, 265 (1988) [Sov. Phys. Usp. **31**, 535 (1988)].
[159] F. Kh. Gel'mukhanov and A. M. Shalagin, Pis'ma Zh. Eksp. Teor. Fiz. **29**, 773 (1979) [JETP Lett. **29**, 711 (1979)].

Translated by S. Chomet